



TAMPERE UNIVERSITY OF TECHNOLOGY  
*Degree Programme in RF Electronics*

**NEBIAT TEKLE AWANO**

**DUAL POLARIZED PATCH ANTENNA FOR UHF RFID READERS**

Master of Science Thesis

Examiners: Adjunct Professor Leena Ukkonen  
and Professor Lauri Sydänheimo.  
Examiners and topic approved in the  
Computing and Electrical Engineering Faculty  
Council meeting on 8 December 2010.

# ABSTRACT

TAMPERE UNIVERSITY OF TECHNOLOGY

Masters Degree Program in Radio Frequency Electronics

**AWANO, NEBIAT TEKLE:** Dual Polarized Patch Antenna for UHF RFID Readers

Master of Science Thesis, 68 pages, 3 appendix pages

December 2010

Major subject: Radio Frequency Electronics

Examiner(s): Adjunct Professor Leena Ukkonen and Professor Lauri Sydänheimo

Key words: Radio Frequency Identification, RFID Technology, polarization, dual polarized Antenna

RFID is a fast emerging automatic identification system. Its bigger data density, better security, high speed and the fact that it does not need mechanical contact or line of sight communication have made it preferable to many other identification systems such as bar code, optical character recognition, biometric identification and smart cards.

Nevertheless, this fast growing technology faces some difficulties in keeping tags simple and low cost while keeping efficient and reliable communication. This thesis is among the solutions that are proposed to fulfill this goal. So far, readers usually have either linearly or circularly polarized antennas and most tags are linearly polarized. Linearly polarized reader antennas are highly sensitive to the orientation of tags. In addition, circularly polarized reader antennas have fields that rotate across a plane and thus have only 50% polarization matching with tags. Accordingly, a dual linearly polarized patch antenna is proposed, implemented and tested as a solution to reduce the power loss caused by an arbitrary orientation of RFID tags.

Among the RFID technologies, passive UHF RFID, which has a bigger read range and simpler tags, working in UHF frequency, is given emphasis in this project. Thus, background information about reader antennas and dual polarized antennas has been made. In addition, a reader antenna based on a patch antenna operating in European UHF RFID band of 865 MHz-868 MHz is considered. The modeling softwares CST Microwave Studio and Empire XCell were used in simulation. Then, the laboratory facility in Electronics department of Tampere University of Technology was used to implement and test the prototype.

## PREFACE

This project was carried out in Tampere University of Technology (TUT), Department of Electronics, RFID Unit from March to October, 2010. It is a research work to come up with dual polarized patch antennas for UHF RFID readers. It is done as a master's thesis at the last stage of my degree in RF Electronics. The topic was introduced to me by my supervisors Adjunct Professor Leena Ukkonen and Professor Lauri Sydänheimo.

First, I would like to thank my supervisors Adjunct Professor Leena Ukkonen and Professor Lauri Sydänheimo for this wonderful opportunity that they have given me and their support throughout the thesis. I would also like to thank researchers Abdul Ali Babar, Tiiti Kellomäki, Toni Björninen and Juha Virtanen for being there for me whenever I get lost. I would also like to thank my teachers: Olli-Pekka Lundén, for his valuable lessons and Jari Kangas for his uninterrupted follow up during the two year time.

Thanks to my peers Karina, Anabel, Sahin and every one in RF Electronics 2008. My heart goes to my family and my parents Abiye and Etiye who have carried me all the way and taught me nothing but love. Last but not least, my sweet Mahi, I love you so much and I am blessed to have you.

Most importantly, I would like to thank God who has been my shepherd, that kept me in green pastures and led me beside the still waters, comforted me with his staff and rod; who shows me the way when I astray and becomes hope when I fail!

Then, I invite you to enjoy reading it ☺

Tampere, November 2010

---

Nebiat Tekle Awano

nebiat20@gmail.com

# CONTENTS

1. INTRODUCTION.....	1
1.1. Scope of the Thesis .....	1
1.2. Outline of the Thesis.....	1
2. ELECTROMAGNETIC THEORY .....	3
2.1. Time Harmonic Forms.....	5
2.2. Generation of Electromagnetic Waves .....	6
2.3. Propagation of Electromagnetic Waves.....	6
2.4. Uniform Plane Waves and Different Wave Modes .....	8
2.5. Electromagnetic Power Transfer .....	9
2.6. Boundary Conditions of Electromagnetic Fields.....	10
3. ANTENNA BASICS .....	11
3.1. Radiation Problem .....	11
3.2. Basic Antenna Parameters .....	12
3.2.1. Radiation Patterns.....	12
3.2.2. Input Impedance .....	13
3.2.3. Quality Factor .....	14
3.2.4. Bandwidth.....	15
3.2.5. Radiation Efficiency .....	15
3.2.6. Average Radiated Power .....	16
3.2.7. Directivity.....	16
3.2.8. Gain .....	17
3.2.9. Polarization.....	18
3.3. Types of Antennas .....	19
4. RECTANGULAR PATCH ANTENNA.....	21
4.1. Analysis Techniques for Microstrip Elements.....	21
4.1.1. Transmission Line Model.....	21
4.1.2. Modal Cavity Model.....	23
4.1.3. Computational Models Used by Simulation Software .....	28
4.2. Characteristics of Rectangular Patch Antennas .....	29
4.2.1. Radiation Fields of Rectangular Patch Antennas .....	29
4.2.2. Bandwidth of Rectangular Patch Antennas .....	30

4.2.3.	Directivity and Gain of Rectangular Patch Antennas.....	31
4.3.	MSA Feed Techniques.....	31
5.	OVERVIEW OF RFID SYSTEMS .....	33
5.1.	RFID as an Automatic Identification System .....	33
5.2.	Classification of an RFID System .....	33
5.3.	Applications of RFID Systems .....	35
5.4.	UHF RFID Systems .....	35
5.5.	Link Budget for a UHF RFID System .....	36
5.6.	Review of Reader Antennas .....	38
5.6.1.	Structure and Feed .....	39
5.6.2.	Polarization.....	40
5.6.3.	Bandwidth.....	40
5.6.4.	Gain .....	40
6.	DUAL POLARIZED ANTENNAS.....	42
6.1.	Polarization Loss Factor .....	42
6.2.	Main Design Considerations of Dual Polarized UHF RFID Patch Antennas ..	44
6.2.1.	Designing the Feeds .....	44
6.2.2.	Isolation.....	46
6.2.3.	Bandwidth.....	46
6.2.4.	Gain .....	46
7.	EXPERIMENTAL ANTENNA.....	47
7.1.	Designing Patch Size .....	47
7.2.	Simulation Results .....	49
7.3.	Measurement Results .....	53
7.4.	Modification of the Basic Antenna.....	57
8.	CONCLUSIONS.....	59
	REFERENCES.....	61
	APPENDIX 1: SURVEY OF KEY PARAMETERS OF SOME DUAL POLARIZED ANTENNAS FROM IEEE PAPERS .....	66
	APPENDIX 2: FR4 SUBSTRATE MATERIAL PARAMETRES.....	68

## SYMBOLS

<b><i>E</i></b>	Electric field intensity (V/m)
<b><i>H</i></b>	Magnetic field intensity (A/m)
<b><i>D</i></b>	Electric flux density (C/m <sup>2</sup> )
<b><i>B</i></b>	Magnetic field density (T, Wb/m <sup>2</sup> )
<b><i>J</i></b>	Electric current density (A/m <sup>2</sup> )
<b><i>A</i></b>	Magnetic vector potential
<b><i>M</i></b>	Magnetic current density
<b><math>\rho</math></b>	Charge density (C/m <sup>3</sup> )
<b><math>\mu</math></b>	Magnetic permeability (H/m)
<b><math>\epsilon</math></b>	Electric permittivity (E/m); $\epsilon_r$ for relative permittivity; $\epsilon_0$ for permittivity in free space
<b><math>\omega</math></b>	Angular speed = $2\pi f$
<b><math>\gamma</math></b>	Propagation constant
<b><math>\alpha</math></b>	Attenuation Constant (Np/m)
<b><math>\beta</math></b>	Phase constant (rad/s)
<b><math>\hat{x}</math></b>	Unit vector in x direction
<b><math>\hat{y}</math></b>	Unit vector in y direction.
<b><math>\sigma</math></b>	Electric conductivity
<b><i>P</i></b>	Power flow into or out of a system; $P_{TX}$ for power transmitted; $P_R$ for received power
<b><i>P</i></b>	Poynting vector (W/m <sup>2</sup> ); $\mathbf{P}_{av}$ for Average power density or Poynting vector (V/m)
<b><i>r</i></b>	distance from source (m) or one of the spherical coordinates ( $\phi, \theta, r$ )
<b><math>\theta</math></b>	theta, one of the spherical coordinates ( $\phi, \theta, r$ )
<b><math>\phi</math></b>	phi, one of the spherical coordinates ( $\phi, \theta, r$ )

$Q$	Quality factor, $Q_t$ for total $Q$ ; $Q_{rad}$ for radiation $Q$ ; $Q_c$ for conduction $Q$ ; $Q_d$ for dielectric $Q$ and $Q_{sw}$ for surface wave $Q$ .
$K$	Constant used to calculate radiation loss and the respective quality factor
$f$	Frequency; $f_0$ or $f_r$ for resonance frequency; $\Delta f$ for difference in maximum and minimum frequencies of interest
$e$	Radiation efficiency, $e_o$ for total efficiency, $e_r$ matching efficiency and $e_{cd}$ for conduction dielectric related efficiency
$\Gamma$	Reflection coefficient (unit less)
$R$	Resistance, $R_L$ resistance accounting for conduction. $R_L$ for radiation resistance
$D(\theta, \phi)$	Directivity
$U(\theta, \phi)$	Radiation Intensity in a given direction ( $\text{W}/\text{m}^2$ ), $U_0$ for Average intensity
$G(\theta, \phi)$	Gain in for a given direction, $G$ for maximum gain
$\hat{u}_{co}$	Co-polarization unit vector
$\hat{u}_{cross}$	Cross polarization unit vector
$G$	Conductance ( $mho$ ), shares symbol with gain
$B$	Susceptance ( $mho$ )
$\lambda$	Wavelength
$z_0$	wave impedance in free space
$k$	Wave number
$t$	Patch antenna thickness
$L, W$	Patch length and width
$A_e$	Aperture area
$q$	Patch antenna fringe constant

## ABBREVIATIONS

AC	Alternating Current
ADS	Advanced Design System; it is RF simulation software.
Auto ID	Automatic Identification
BW	Bandwidth
CST MWS	CST Microwave Studio, simulation software used in the project
DC	Direct Current
EIRP	Effective Isotropic Received Power. It is the amount of power an isotropic antenna would need in order to produce equivalent radiation with that of a directional antenna.
EM	ElectroMagnetic
FDTD	Finite Difference Time Domain, a method to solve differential time domain Maxwell's Equations
FIT	Finite Integration Technique, a method used to solve Maxwell's equations
HF	High Frequency, the frequency range covering 3 MHz-30 MHz in the electromagnetic spectrum
IC	Integrated Circuit
ISM	Industrial, Scientific and Medical, a frequency band reserved for these purposes
LF	Low Frequency, the frequency range of 30 KHz-300 KHz in the electromagnetic spectrum
LNA	Low Noise Amplifier, an amplifier usually put in the front end of receiver circuits to amplify very sensitive signals
MSA	Microstrip Antennas
PEC	Perfect Electric Conductor
PLF	Polarization Loss Factor
RF	Radio Frequency

RFID	Radio Frequency Identification, a generic term for technologies that use electromagnetic coupling and radio waves to identify objects or people
S Parameters	Scattered Parameters, one method of describing the network parameters with respect to power waves.
TEM	Transverse Electric and Magnetic mode: a transmission mode in transmission lines and free space where electric and magnetic fields are orthogonal with each other and with the direction of propagation.
TE	Transverse Electric mode, a transmission mode in waveguides that have only the electric field vector perpendicular to the direction of propagation.
TM	Transverse Magnetic mode, a transmission mode in waveguides that have only the magnetic field vector perpendicular to propagation.
TUT	Tampere University of Technology
UHF	Ultra High Frequency, a frequency range covering from 300 MHz - 3 GHz in the electromagnetic spectrum.
VNA	Vector Network Analyzer, a measurement device used to measure circuit network parameters, commonly scattering parameters.
VSWR	Voltage Standing Wave Ratio, a ratio of the maximum to minimum of a standing voltage wave obtained from reflection because of impedance mismatch.

# 1. INTRODUCTION

Radio Frequency Identification (RFID) is a class of automatic identification technologies that use electromagnetic fields or radio waves to detect objects animals or people. A generic RFID system consists of wireless communication between a transponder or a tag that is placed on the object to be identified and a reader.

This thesis focuses on passive UHF (Ultra High Frequency) RFID systems. The term passive is to indicate that the tag does not have a complete transceiver circuit and a battery of its own; instead it consists of a chip to store and process data and an antenna to receive and transmit radio frequency power. Therefore, passive RFID tags use the radio frequency power coming from the reader to activate the chip as well as to communicate back to the reader.

Consequently, maximizing the possibility of getting bigger read range while keeping small size and low cost tags requires designs of energy efficient RFID systems. This has been the interest of the RFID industry. Several novel designs of tag and reader antennas have been proposed. This thesis proposes using dual polarized reader antennas to reduce power lost due to polarization mismatch. So far, the reader antennas in use commonly have linear or circular polarizations and have bigger polarization mismatches.

The thesis compares several fixed reader antennas and dual polarized antennas. Finally a novel dual polarized antenna to work in the European RFID band or 865 MHz – 868 MHz is proposed. Simulations are carried out using Empire XCcell and CST Microwave Studio. The antenna is implemented, modified and measured in RF workshop lab, Satimo Starlab and tagformance tag environment of Electronics Department of Tampere University of Technology.

## 1.1. Scope of the Thesis

The thesis is limited to discussing basic electromagnetic science, antenna and microwave engineering. Overview of RFID technology is also given. In fact, focus is given to passive UHF RFID technology with fixed readers.

The designed patch antenna is also limited to academic purpose and has a narrow band to work in the European RFID band.

## 1.2. Outline of the Thesis

There are a total of eight chapters including the Introduction in the thesis. Chapter 2 discusses overview of the electromagnetic theory. RFID communication is an

electromagnetic phenomenon. Maxwell's equations in differential and integral forms are given. Time harmonic forms were introduced to be used in the rest of the discussions. Generation and propagation of electromagnetic waves is also discussed along with lossy and lossless media. In addition, power electromagnetic power transfer and Poynting theorem are discussed. Finally, boundary conditions are generally illustrated. Their understanding is important in patch antenna models and simulations.

Chapter 3 gives overview about antennas. It begins by stating an antenna problem which is solving the field values for the given current distribution in an antenna. Then, basic qualities that characterize an antenna are defined. These are radiation pattern, input impedance, bandwidth quality factor, efficiency, directivity and gain. Polarization is discussed at last. Co-polarization and cross polarization are then defined. Good antennas have low cross polarization. Chapter 3 is finalized discussing the different antenna types.

Chapter 4 specializes in Microstrip Antennas (MSAs). Most of the chapter discusses the analysis models for patch antennas: transmission line model, modal cavity model and models used in simulation softwares. The second section discusses MSA characteristics such as radiation patterns, bandwidth, gain and feeding techniques.

Chapter 5 revises the RFID technology with emphasis on passive UHF RFID systems. First RFID is compared with other identification systems. Then, classification of RFID systems is given. Besides, UHF RFID systems are discussed. The chapter finally shows survey of antennas for fixed readers with regard to key parameters such as bandwidth, gain, polarization and feed structures.

In Chapter 6 dual polarized antennas are discussed in detail. Most of the comparison is done from antennas proposed in International Electrical and Electronics Engineers (IEEE) papers. In the first part the chapter answers the key question "why go for a dual polarized antenna?" The chapter finally finishes by comparing the major design obstacles in dual polarized MSAs: isolation and bandwidth.

In chapter 7, the experimental dual polarized patch antenna for UHF RFID readers is proposed and illustrated. First the initial design steps such as designing the patch are mentioned. The proposed antenna and its means of coupling is shown. The chapter then proceeds by showing the simulated and measured results for the basic and modified antennas.

Conclusion, chapter 8 is given in the last chapter. The successes, limitations and future research ideas are given in this chapter.

## 2. ELECTROMAGNETIC THEORY

Microwave frequencies generally range from 300 MHz-3 GHz or wavelengths from 1mm-1m. Most topics of microwave engineering including antenna design are based on finding solutions for Maxwell's equations for different material and geometrical settings for different excitation conditions. The following four equations are called Maxwell's equation, named after James Clerk Maxwell. [1; 2; 36]

$$\nabla \times \mathbf{E} = -\frac{\partial \mathbf{B}}{\partial t} \quad (2.1)$$

$$\nabla \times \mathbf{H} = \mathbf{J} + \frac{\partial \mathbf{D}}{\partial t} \quad (2.2)$$

$$\nabla \cdot \mathbf{D} = \rho \quad (2.3)$$

$$\nabla \cdot \mathbf{B} = 0 \quad (2.4)$$

To make these equations complete, one more equation - known as the equation of continuity, is used. Its importance is mentioned in the subsequent discussion.

$$\nabla \cdot \mathbf{J} = -\frac{\partial \rho}{\partial t} \quad (2.5)$$

Here,  $\mathbf{E}$  stands for the electric field intensity,  $\mathbf{B}$  stands for magnetic flux density,  $\mathbf{H}$  stands for magnetic field intensity,  $\mathbf{J}$  stands for conduction current density and  $\mathbf{D}$  stands for electric flux density. The same symbols are used throughout the thesis. The above equations are constituted by the relations  $\mathbf{D} = \epsilon \mathbf{E}$  and  $\mathbf{B} = \mu \mathbf{H}$  where  $\epsilon$  stands for the electric permittivity and  $\mu$  represents the magnetic permeability. [3]

Equations (2.1)-(2.4) are called the differential forms of Maxwell's equations. The first equation is called Faraday's law and it says that a curly electric field produces a time varying magnetic field. The second equation is modified from Ampere's circuital law and says a rotational magnetic field gives an electric current. (2.3)- (2.4) are called Gauss electrostatic and magnetostatic laws. We can see that magnetic fields are solenoidal because there are no magnetic charges where as the divergence of electric flux density gives the total electric charge density.

Maxwell's equations rather give more meaning when written in integral forms. Their integral counterparts are obtained by taking integrals of both sides and using

divergence and Stokes's theorem and are shown below. First let us see Faraday's law. Faraday's law in integral form is given in equation 2.6.

$$\oint_{\partial S} \mathbf{E} \cdot d\mathbf{l} = - \iint \mathbf{B} \cdot \mathbf{n} dS \quad (2.6)$$

The line integral  $\oint_{\partial S} \mathbf{E} \cdot d\mathbf{l}$  is a closed integral on the surface  $\partial S$  and it equals the electromotive force induced across the closed contour. If the contour is in vacuum or a dielectric, then the electric field exists with the force whereas the effect is pronounced and easily seen for a conductor when the force induces current across the conductor. For non zero  $\mathbf{E}$ , the term  $\oint_{\partial S} \mathbf{E} \cdot d\mathbf{l}$  will be zero for irrotational fields which is the case for electrostatic fields. [2]

Next is shown Ampere's law in integral form.

$$\oint_{\partial S} \mathbf{H} \cdot d\mathbf{l} = \iint_S \left( \mathbf{J} + \frac{\partial \mathbf{D}}{\partial t} \right) \cdot \mathbf{n} dS \quad (2.7)$$

Ampere's original idea was taken from Hans Christian Ørsted's experiment where a magnetic needle reflects nearby a current carrying conductor and it states that the contour integral of the magnetic field gives the steady state current enclosed by the contour, i.e. [1]

$$\oint_{\partial S} \mathbf{H} \cdot d\mathbf{l} = \iint_S \mathbf{J} \cdot \mathbf{n} dS \quad (2.8)$$

On the contrary, according to Maxwell, this is inconsistent with the law of conservation of charge which is stated in (2.5) above or in integral form it is,

$$\iint_S \mathbf{J} \cdot \mathbf{n} dS = - \frac{\partial}{\partial t} \iiint_V \rho dv \quad (2.9)$$

In simple terms, the total outward flow of charge from a surface enclosing a volume is accompanied by the total change of charge in the volume. Therefore, it can be seen that (2.8) implies  $\nabla \times \mathbf{H} = \mathbf{J}$  and if we take the divergence of both we get null on the left side which implies  $\nabla \cdot \mathbf{J} = 0$  in contradiction to the conservation of charge equation shown in (2.5). To account for this, Maxwell introduced the term  $\frac{\partial \mathbf{D}}{\partial t}$ , referred to as the convection current in the right side as shown in (2.7) [1]

Next is shown the integral form of Gauss law, which more than the differential form directly implies that the total flux entering a surface enclosing a volume equals the total charge in the volume.

$$\iint_{\partial V} \mathbf{D} \cdot \mathbf{n} dS = Q \text{ (total charge in } V) \quad (2.10)$$

On the other hand the magnetostatic Gauss law shows that there is no flux leaving any volume.

$$\iint_{\partial V} \mathbf{B} \cdot \mathbf{n} dS = 0 \quad (2.11)$$

So far, we have seen the guiding equations of electromagnetism and their physical meaning. Now let us see more about the generation and transfer of electromagnetic fields, wave and power.

## 2.1. Time Harmonic Forms

Time harmonic sinusoidal functions have widespread use in electrical engineering. In addition, an arbitrary signal can be represented as a Fourier combination of time harmonic sinusoidal functions. As a result, making use of time harmonic functions simplifies the analysis of Maxwell's equations. Besides, Maxwell's equations are linear differential equations and the sinusoidal variation of the sources ( $\mathbf{J}, \rho$ ) produces  $\mathbf{E}$  and  $\mathbf{H}$  fields of sinusoidal functions in the same frequency which produce further simplification [2].

To ease the analysis of differential equations, complex domain is used. Then, these sinusoidal functions are represented with phasors quantities showing amplitude and phase. Field vectors that are functions of spatial coordinates and sinusoidal functions of time can also be represented by phasors of spatial coordinates. For instance, the instantaneous  $\mathbf{E}$  field  $\mathbf{E}(x, y, z; t)$ , can be represented by its corresponding vector phasor  $\mathbf{E}(x, y, z)$ , as [2]

$$\mathbf{E}(x, y, z; t) = \text{Re}[\mathbf{E}(x, y, z)e^{j\omega t}] \quad (2.12)$$

Now we can see, if we replace  $\mathbf{E}(x, y, z; t)$  by  $\mathbf{E}(x, y, z)$ , then  $\frac{\partial \mathbf{E}(x, y, z; t)}{\partial t}$

is replaced by  $j\omega \mathbf{E}(x, y, z)$ . With this logic in mind, Maxwell's differential equations with  $\mathbf{E}$  and  $\mathbf{H}$  can be rewritten as

$$\nabla \times \mathbf{E} = -j\omega\mu\mathbf{H} \quad (2.13)$$

$$\nabla \times \mathbf{H} = \mathbf{J} + j\omega\epsilon\mathbf{E} \quad (2.14)$$

$$\nabla \cdot \mathbf{E} = \frac{\rho}{\epsilon} \quad (2.15)$$

$$\nabla \cdot \mathbf{H} = 0 \quad (2.16)$$

## 2.2. Generation of Electromagnetic Waves

Let us look at Faraday's and Ampère's equations.

$$\nabla \times \mathbf{E} = -\frac{\partial \mathbf{B}}{\partial t} \quad (2.17)$$

$$\nabla \times \mathbf{H} = \mathbf{J} + \frac{\partial \mathbf{D}}{\partial t} \quad (2.18)$$

As mentioned before,  $\mathbf{D} = \epsilon\mathbf{E}$  and  $\mathbf{B} = \mu\mathbf{H}$ . Under normal circumstances we deal with constant permittivity and permeability [3]. This grants constant proportionality between  $\mathbf{D}$ ,  $\mathbf{E}$  and  $\mathbf{B}$ ,  $\mathbf{H}$ . Therefore, in 2.17, to have a curly  $\mathbf{E}$  field, we have to have a time varying  $\mathbf{B}$ , which can be obtained from a time varying current. Then, we see 2.18 works because we already said of the existence of current,  $\mathbf{J} + \frac{\partial \mathbf{D}}{\partial t}$ , so we will have a curly  $\mathbf{H}$  field as well. The necessary assumption we made here is the presence of a time varying current. Consequently, we see only accelerated charges produce radiations.

There are many ways to accelerate charges. A material that has static charges does not radiate. If charges are moving in a uniform motion to produce radiation the material has to be bent or oriented to accelerate the charges. Discontinuities in materials also force charge acceleration. However, a rather common means of acceleration of charges that has tremendous applications is supplying an alternating current. [4]

## 2.3. Propagation of Electromagnetic Waves

Maxwell's equations can be solved for a generic linear and isotropic generic medium. For such medium the homogeneous wave equations are [2]

$$\nabla^2 \mathbf{E} + \gamma^2 \mathbf{E} = 0 \quad (2.19)$$

$$\nabla^2 \mathbf{H} + \gamma^2 \mathbf{H} = 0 \quad (2.20)$$

where,  $\gamma$  stands for the complex propagation constant.

$$\gamma = \alpha + j\beta \quad (2.21)$$

$\beta$  is called a phase constant of the propagating wave and

$$\beta = \omega^2 \epsilon \mu \quad (2.22)$$

$\alpha$  accounts for the loss in propagation distance and depends on material characteristics. For lossless media  $\alpha = 0$ . The following figure illustrates the effect of  $\alpha$ .

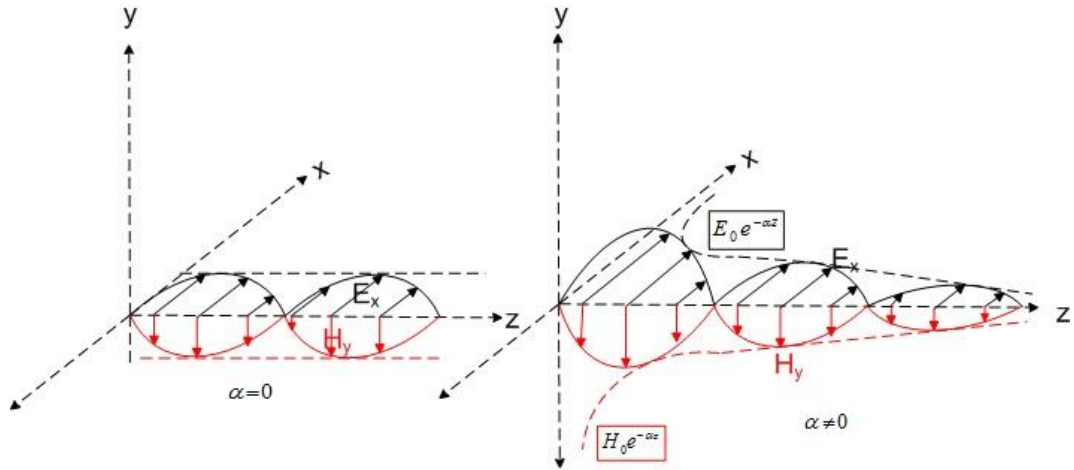


**Fig. 2.1** Wave propagating in lossless medium (left) and lossy medium (right)

As can be seen from fig. 2.1 above, for a lossless media ( $\alpha = 0$ ) in the left, the amplitude remains constant. This is the case for perfect dielectrics such as vacuum. Propagation in a lossy media is shown in the right. Here,  $\alpha \neq 0$ , there is an exponential decay in the peak amplitudes  $E_0$  and  $H_0$ . Propagation in metals or other conductors is a good example for this. Usually, the effect is given such that the amplitude is reduced by the factor  $\frac{1}{e}$  and this distance is called skin depth and it is given as,

$$\delta = \frac{1}{\alpha} \quad (2.23)$$

## 2.4. Uniform Plane Waves and Different Wave Modes

Once, a wave is far from the source, it propagates perpendicular to a certain plane where all the fields will be oriented parallel to the plane and the fields can be considered the same throughout the plane.  $\mathbf{E}$  and  $\mathbf{H}$  will be perpendicular and the same throughout the plane. Such waves are defined as uniform plane waves and such modes are called transverse electromagnetic (TEM) waves. For the sake of simplification, one of the Cartesian coordinate axes is used as the direction of propagation and the remaining two orthogonal axes will be the directions of  $\mathbf{E}$  and  $\mathbf{H}$ . [2; 3]

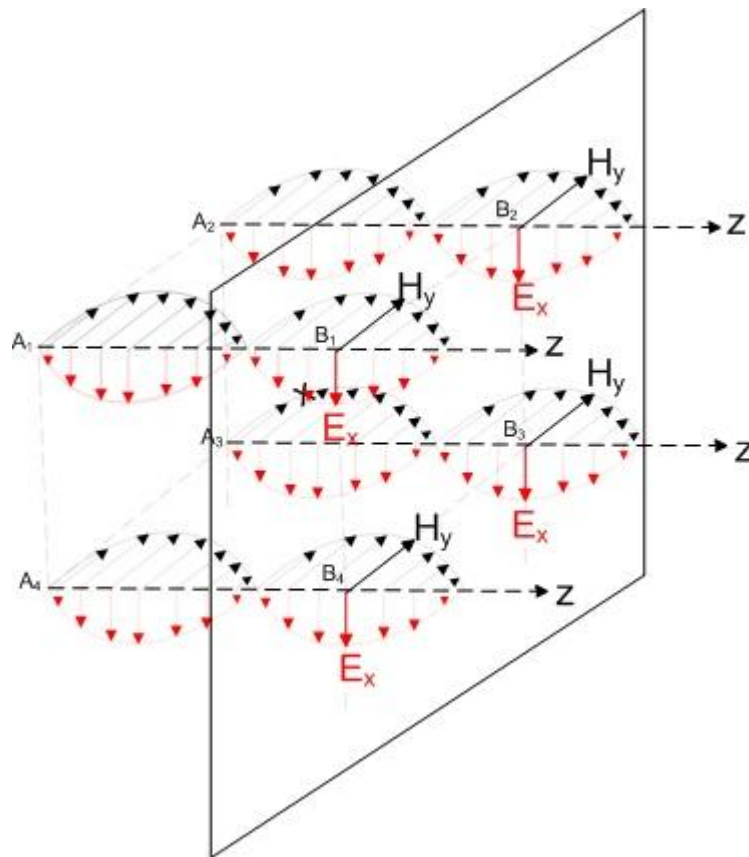


**Fig. 2.2** Plane wave propagating in a lossless media. The fields in bold are projected on the plane in four points

Fig. 2.2 above shows a plane wave with field directions  $\mathbf{E}_x$  and  $\mathbf{H}_y$  propagating in  $z$  direction. Four “rays”, as components of the plane wave, originate from points  $A_1$ ,  $A_2$ ,  $A_3$  and  $A_4$  and are projected on the plane at  $B_1$ ,  $B_2$ ,  $B_3$  and  $B_4$ . The fields are equated as

$$\mathbf{E}_x = \mathbf{E}_0 e^{-\gamma z} \hat{\mathbf{x}} \quad (2.24)$$

$$\mathbf{H}_y = \mathbf{H}_0 e^{-\gamma z} \hat{\mathbf{y}}$$

$E_0$  and  $H_0$  stand for the maximum  $E_x$  and  $H_y$  respectively.  $\gamma$  stands for the complex propagation constant.

TEM modes are not the only modes electromagnetic waves can exist. In wave guides TEM modes do not exist. Instead, there are Transverse Electric (TE) modes and Transverse Magnetic (TM) modes. TE modes have only the electric field orthogonal to the direction of propagation. Similarly, TM modes have the magnetic field component transverse to the direction of propagation. [2; 3]

## 2.5. Electromagnetic Power Transfer

Electromagnetic waves transport power. Using Maxwell's equation and vector identities, the following relation can be obtained. [2; 3]

$$\oint_S \mathbf{E} \times \mathbf{H} \cdot d\mathbf{S} = -\frac{\partial}{\partial t} \int_V \left( \frac{1}{2} \epsilon E^2 + \frac{1}{2} \mu H^2 \right) - \int_V \sigma E^2 dv \quad (2.25)$$

This basically can be interpreted as The electromagnetic power flowing into a surface  $S$  enclosing a volume  $V$  equals the change in magnetic and electric energy plus the total Ohmic loss in the volume. The term  $\mathbf{P} = \mathbf{E} \times \mathbf{H}$  is the power density in watts per square meter called Poynting vector. It is a vector whose direction shows the direction of electromagnetic power flow. [1; 2; 3]

For DC circuits, it has been shown above that direct currents do not radiate owing to no oscillating electric and magnetic energies i.e.  $\frac{\partial}{\partial t} \int_V \left( \frac{1}{2} \epsilon E^2 + \frac{1}{2} \mu H^2 \right) = 0$ . The  $\mathbf{E} \times \mathbf{H}$  term equals the Ohmic loss term,  $\sigma E^2$ . What we just considered is actually a DC situation in a conductor because if the conductivity was zero, we would not have the  $H$  term in the first place; implying no  $\mathbf{E} \times \mathbf{H}$ . On the other hand, in AC, we will have propagating electromagnetic waves. The  $\int_V \sigma E^2 dv$  term will now be the loss implying that conductors attenuate EM waves where as non conductors keep it in oscillating electric and magnetic energy. [2]

In dealing with time harmonic EM waves, the instantaneous value of a quantity is the real part of the product of the phasor quantity and  $e^{j\omega t}$  when  $\cos\omega t$  is used as a reference. [5]

$$\mathbf{P}(z, t) = \mathbf{E}(z, t) \times \mathbf{H}(z, t) = \text{Re}[\mathbf{E}(z)e^{j\omega t}] \times \text{Re}[\mathbf{H}(z)e^{j\omega t}] \quad (2.26)$$

$$\mathbf{P}_{av}(z, t) = \frac{1}{2} \text{Re}[\mathbf{E}(z) \times \mathbf{H}^*(z)] \quad (2.27)$$

The term  $\frac{1}{2}\mathbf{E}(z) \times \mathbf{H}^*(z)$  is the complex power density. The average Poynting vector is used to calculate the electromagnetic power emanating out of an enclosed volume. i.e. [4]

$$P = \oint_S \mathbf{P}_{av} \cdot d\mathbf{S} = \frac{1}{2} \text{Re} \left[ \oint_S \mathbf{E}(z) \times \mathbf{H}^*(z) \cdot d\mathbf{S} \right] \quad (2.28)$$

## 2.6. Boundary Conditions of Electromagnetic Fields

Boundary conditions describe the relation between electromagnetic fields as a wave crosses a material boundary. The boundary condition for the four field components can be generalized as [2]

$$\mathbf{a}_n \times (\mathbf{E}_2 - \mathbf{E}_1) = \mathbf{0} \quad (2.29)$$

$$\mathbf{a}_n \times (\mathbf{H}_2 - \mathbf{H}_1) = \mathbf{J}_s \quad (2.30)$$

$$\mathbf{a}_n \cdot (\mathbf{D}_2 - \mathbf{D}_1) = \rho_s \quad (2.31)$$

$$\mathbf{a}_n \cdot (\mathbf{B}_2 - \mathbf{B}_1) = 0 \quad (2.32)$$

The field vectors with subscript 1 and 2 stand for field values in medium one and two respectively.

### 3. ANTENNA BASICS

IEEE terms and definitions for antennas defines an antenna as “that part of a transmitting or receiving system that is designed to radiate or receive electromagnetic waves.” Since, antennas are passive reciprocal devices; their reception is implicitly understood from their radiation characteristics. The chapter begins with radiation problem. Then, fundamental antenna parameters and types are discussed. [7]

#### 3.1. Radiation Problem

Antenna radiation problem involves finding the values for  $\mathbf{E}$  and  $\mathbf{H}$  fields that are created as a result of an impressed (source) current,  $\mathbf{J}$ . [6]. Some of the methods of creating the impressed current are discussed with respect to microstrip antennas in chapter 4. For now, let us focus on finding the solution once we have  $\mathbf{J}$ . Using the curl equations from Maxwell’s equations is enough. We know from Gauss law that

$$\nabla \cdot \mathbf{H} = 0 \quad (3.1)$$

Using the vector identity  $\nabla \cdot \nabla \times \mathbf{A} = 0$ , we have a vector potential  $\mathbf{A}$ , such that

$$\mathbf{H} = \frac{1}{\mu} \nabla \times \mathbf{A} \quad (3.2)$$

Replacing equation 2.2 in equation 2.13, we get

$$\nabla \times (\mathbf{E} + j\omega\mathbf{A}) = 0 \quad (3.3)$$

Now we see that from (2.2) and implicitly (2.3) we can calculate  $\mathbf{E}$  and  $\mathbf{H}$  from  $\mathbf{A}$ . Therefore, it is sufficient to find the solution for the potential functions. Accordingly substituting the terms in Maxwell’s equations by  $\mathbf{A}$  and using vector identities, we get [3; 6]

$$\nabla^2 \mathbf{A} + \omega^2 \epsilon \mu \mathbf{A} = -\mu \mathbf{J} \quad (3.4)$$

Equation 2.4 is a vector wave equation which is a differential equation for the given value of  $\mathbf{J}$ . In Cartesian coordinate plane, it consists of three independent equations - one for each coordinate.

The total vector potential  $\mathbf{A}$ , is then calculated as, [3; 6]

$$\mathbf{A} = \iiint_{v'} \frac{\mathbf{J}\mu e^{-j\beta r}}{4\pi r} dv' \quad (3.5)$$

Equation (3.5) can be modified to a given current and geometric distribution to solve the antenna problem. For instance if we take an ideal dipole directed in z direction, the volume integral reduces to a linear integral along an infinitesimal length  $\Delta z$ .

The values for the  $\mathbf{E}$  and  $\mathbf{H}$  fields, also called the radiated fields are then solved according to (2.2) and (2.3) or once  $\mathbf{H}$  is solved,  $\mathbf{E}$  can be solved from Ampere's law as shown in equation 2.13 and for far field as we can ignore  $\mathbf{J}$ . It should be noted that the choice of suitable coordinate plane is decisive to solve the problem easily.

The power and power density flowing out of a volume enclosing the antenna can be calculated with the relation given in section. An imaginary power density corresponds to standing waves, rather than travelling waves which are associated with radiation. Therefore, imaginary power indicates stored energy just as in any reactive device. Depending on the distance from the antenna the values for  $\mathbf{E}$ ,  $\mathbf{H}$  and  $\mathbf{S}$  (power density) are referred to as near field and far field values. [4; 6]

## 3.2. Basic Antenna Parameters

An antenna is characterized by several parameters. Antenna design means optimizing such characteristics for the needed application. Some of these parameters are radiation pattern, input impedance, quality factor, bandwidth, radiation efficiency, average radiated power, directivity, gain and polarization. Each of these is discussed in this section.

### 3.2.1. Radiation Patterns

IEEE antenna terms and definitions defines radiation pattern as “the spatial distribution of a quantity that characterizes the electromagnetic field generated by an antenna.” [7]

The quantities represented in radiation patterns are usually power flux density, radiation intensity, directivity, phase, polarization, and electric or magnetic field strength. The quantities could be mathematically represented but graphical representation is rather common. [7]

The quantities could be given in one, two or three dimensions. 1D and 3D representations are common. In 1D representation, one of the quantities mentioned above is plotted against  $\theta$ , for constant  $\phi$  or vice versa. Usually the planes to plot with are called principal E and principal H plane. “Principal E plane for a linearly polarized antenna is the plane containing the electric field vector and the direction of maximum radiation.” The same definition follows for the principal H plane with respect to the magnetic field vector. [4; 7]

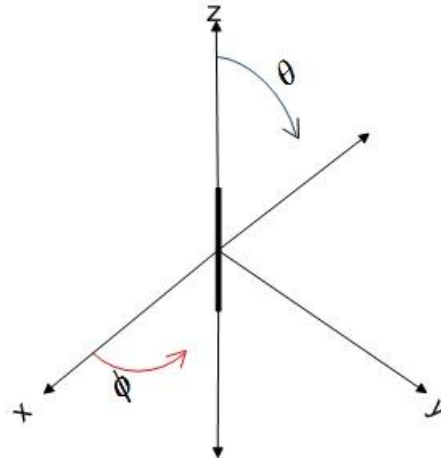


*Fig 3.1 Spherical coordinate plane and principal E and H planes*

Another option is picking the  $xy$  plane called the azimuth plane and the  $yz$  plane or the elevation as shown for an antenna positioned in the figure above. Usually (as it is in the figure) the  $xy$  plane will have the principal H plane and they  $yz$ -plane will have the principal E plane if the antenna is positioned to have its maximum gain to the  $y$  axis. It should be noted that this definition should be modified to cope up with the orientation of the antenna in coordinate system in use.[4; 6; 7]

### 3.2.2. Input Impedance

An antenna can be modeled as a current source with series input impedance. [6]

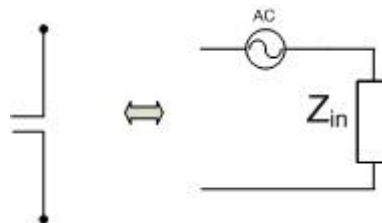


*Fig. 3.2 Equivalent circuit of antennas*

Here,  $Z_{in}$  is called the input impedance of the antenna. In general antenna input impedance is a complex quantity that has real and imaginary parts that depend on frequency. Theoretically both the resistance and the reactance exhibit symmetry about the resonant frequency. The real parts account for the radiated power and the

power lost due to conduction; meanwhile the imaginary parts account for the reactive power returning back to the source.

Impedance matching is a significant part of all antenna designs as long as maximum power transfer is concerned. Proper matching requires that antenna input impedance equals the complex conjugate of the source/feed impedance.[4; 8; 10]

$$Z_{in} = Z_{feed}^* \quad (3.6)$$

Using 50  $\Omega$  terminations in different communication blocks has been the standard. Therefore, most antenna designs take the goal of making the impedance at 50  $\Omega$  in the needed bandwidth. [8]

### 3.2.3. Quality Factor

Is  $2\pi$  times the energy stored in the fields excited by the antenna to the energy radiated and dissipated per cycle. [7] It is a figure of merit that is a representative of antenna losses namely: radiation, conduction (ohmic), dielectric and surface wave losses. The total quality factor is then represented as, [9]

$$\frac{1}{Q_t} = \frac{1}{Q_{rad}} + \frac{1}{Q_c} + \frac{1}{Q_d} + \frac{1}{Q_{sw}} \quad (3.7)$$

$$Q_d = \frac{1}{\tan\delta} \quad (3.8)$$

$$Q_c = h\sqrt{\pi f \mu \sigma} \quad (3.9)$$

$$Q_{rad} = \frac{2\omega\epsilon_r}{h\frac{G_t}{l}} K \quad (3.10)$$

$\frac{G_t}{l}$  stands for conductance per length and

$$K = \frac{\iint_{area} |E|^2 dA}{\oint_{perimeter} |E|^2 dl} \quad (3.11)$$

As can be seen from the equations above,  $Q_{rad}$  is inversely proportional to the substrate width,  $h$  and so for very thin substrates, it is the dominant factor.

### 3.2.4. Bandwidth

Bandwidth is usually defined as [4]

$$BW = \frac{\Delta f}{f_0} = \frac{1}{Q_t} \quad (3.12)$$

The value may then be given in percent. This definition is modified a little bit for MSAs because it does not take into account the impedance matching at the input terminals of the antenna. A more relevant definition is given in the next chapter. [4]

### 3.2.5. Radiation Efficiency

The radiation efficiency of an antenna is a merit that takes into account the losses at the input terminals and within the structure of the antenna. Losses at the input terminals are caused because of reflection caused by impedance mismatch with the feed or  $I^2R$  loss. Losses within the structure account for conduction and dielectric losses. The overall radiation efficiency can be written as [4]

$$e_0 = e_r e_{cd} \quad (3.13)$$

where  $e_0$  is the total radiation efficiency,  $e_r = 1 - |\Gamma|^2$  is the reflection (mismatch efficiency).  $e_{cd}$  is conduction-dielectric efficiency, mathematically (as a consequence of the long power relation).

$$e_{cd} = \frac{R_r}{R_r + R_L} \quad (3.14)$$

Where  $R_r$  represents radiation losses and  $R_L$  is a resistance to represent the conduction- dielectric losses. Usually  $e_{cd}$  itself is regarded as antenna efficiency since if the reflection is considered independently.  $e_{cd}$  can be given interms of quality factors for an MSA as, [4]

$$e_{cd} = \frac{Q_t}{Q_{rad}} \quad (3.15)$$

### 3.2.6. Average Radiated Power

Poynting vector, as defined in section 2.5, represents the power flow density. The average radiated power ( $P_{rad}$ ) out of a volume thus is calculated by integrating the Poynting vector coming out of the volume. [2; 4; 6]

$$P_{rad} = \iint \mathbf{P}_{av} \cdot d\mathbf{S} \quad (3.16)$$

The radiation intensity then is defined as “the ratio of the total power radiated by from an antenna per unit solid angle”. [7]

$$U(\theta, \phi) = R^2 \mathbf{P}_{av} \quad (3.17)$$

### 3.2.7. Directivity

“Directivity of an antenna in a certain direction is the ratio of the radiation intensity in that direction to the radiation intensity of the antenna averaged in all directions. The average intensity,  $U(\theta, \phi)$  equals the total power radiated,  $P_{rad}$ , divided by  $4\pi$ .” [7]

$$D(\theta, \phi) = \frac{U(\theta, \phi)}{U_0} = \frac{4\pi U(\theta, \phi)}{P_{rad}} \quad (3.18)$$

The value calculated in equation 3.18 is the directivity pattern for different values of  $(\theta, \phi)$ . If a single number is used to see the figure of merit, then the number stands for the maximum directivity. This number is usually expressed in dB.

The figure below compares the polar radiation patterns of an isotropic and a certain directive antenna. An isotropic radiator is “a hypothetical lossless antenna having equal radiation intensity in all directions [7]”. Directive antennas have one or more main lobe and may have side lobes and back lobe. As can be seen from fig. 3.3, a directional antenna has power concentrated in certain directions. If a lossless directional antenna and an isotropic antenna are considered, their total power taken throughout the region will be the same.

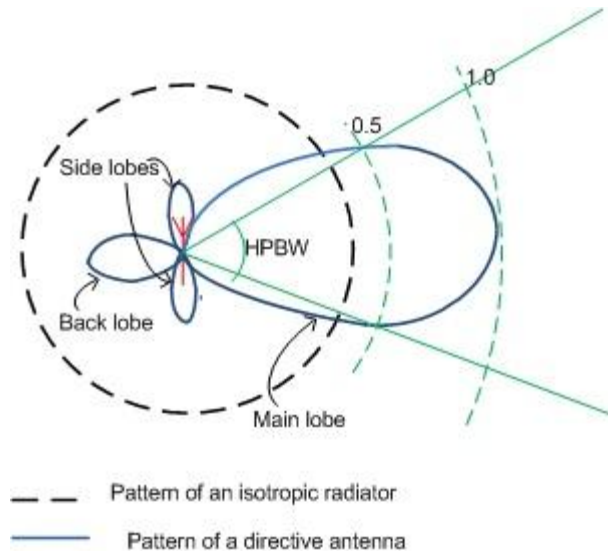


*Fig. 3.3 Comparison of a directive antenna with an isotropic radiator.*

Half Power Beam Width (HPBW) equals the angle the power is reduced by 3 dB from the maximum.

### 3.2.8. Gain

The gain of the antenna is the directivity including other losses. If an antenna is without dissipative loss, then in any given direction, its gain is equal to its directivity. [7] Mathematically,

$$G(\theta, \phi) = e_{cd}D(\theta, \phi) \quad (3.19)$$

Gain is usually expressed relative to an ideal isotropic antenna (dBi) [10]. However, gain optimization needs the concept of EIRP (Effective Isotropic Received Power). For a certain directional antenna, we have an EIRP that an isotropic antenna would need in order to produce equivalent radiation. [10]

$$EIRP = P_{TX}(dB) + G_{TX}(dB) \quad (3.20)$$

The reason for specifying EIRP is because standards refer to EIRP. For instance in the US an antenna of peak power 1W (30 dBm) with gain of 6 dBi is allowed for each 1 dB of antenna gain increase the peak power has to be reduced by 1 dB [10]. That way the EIRP is maintained constant

### 3.2.9. Polarization

Polarization of a wave radiated by an antenna indicates the direction and magnitude characteristics of the electric field vector as it propagates in the given direction. When the direction is not stated, the polarization is taken to be the polarization in the direction of maximum gain. [7]

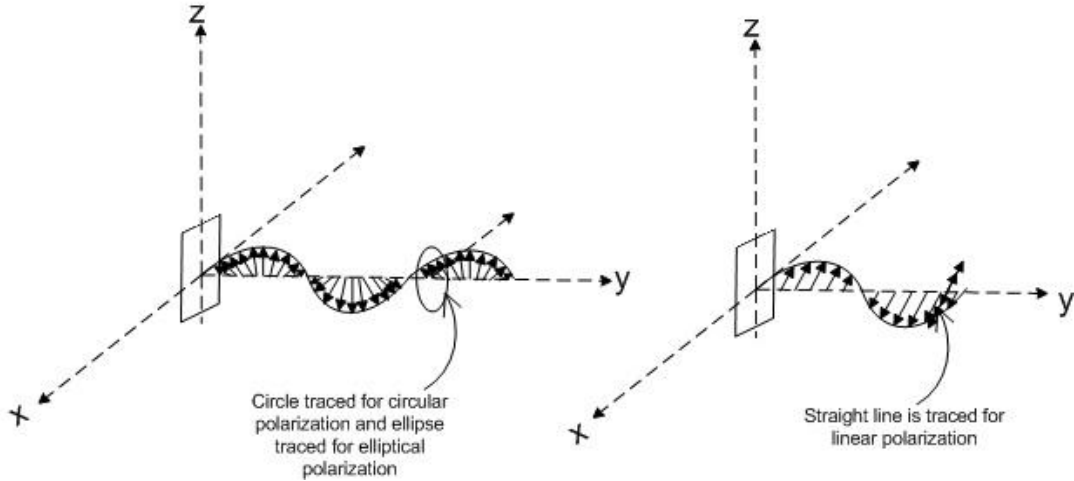


**Fig. 3.4** Illustration of linear, circular and elliptical polarizations.

When the wave radiated from an antenna propagates, it draws a picture on the plane perpendicular to its propagation- a line, a circle or an ellipse. The use of orthogonal polarization to provide two communications channels for each frequency band has led to interest in polarization purity. Co-polarization is as the polarization that an antenna is desired to radiate and cross polarization is the polarization orthogonal to co-polarization [7].

There have been different definitions of reference planes for cross and co-polarization. One way according to Ludwig [11] in rectangular or spherical coordinate system assigning one unit vector as co-polarization and the other as cross polarization. But a more meaningful definition to linear antennas is given by Ludwig known as Ludwig 3. [11]

$$\begin{aligned}\hat{u}_{co} &= \sin(\phi)\hat{\theta} + \cos(\phi)\hat{\phi} \\ \hat{u}_{cross} &= \cos(\phi)\hat{\theta} - \sin(\phi)\hat{\phi}\end{aligned}\quad (3.21)$$

Where  $\hat{u}_{co}$  stands for the co polar vector and  $\hat{u}_{cross}$  stands for the cross polar vector. Depending on the direction of electric field excitation mode, vertical and horizontal polarization have to be linked with cross polarization and co-polarization. For instance if we assume the vertical component as y-direction (in Cartesian coordinate), then if we have  $E_y$  as the main waveguide mode component, then co-polarization is identical to  $E_{vertical}$  and cross polarization is identical to  $E_{horizontal}$ . [12]

### 3.3. Types of Antennas

Antennas could be divided based on different grounds. One way of classifying them is mainly with their size and bandwidth. Stutzman classifies them as follows [6].

1. Electrically Small Antennas: Antennas such as short dipoles and loop wires. The loops can take other shapes such as ellipse, rectangle, etc.



**Fig. 3.5** Examples of electrically small antennas small dipole (left) and small loop (right)

Electrically small antennas are characterized by small radiation resistances and bigger loss resistances. Therefore, they have small gain. They also have narrow bandwidth.

2. Resonant Antennas: half wave dipole and patch antenna are best examples of resonant antennas.

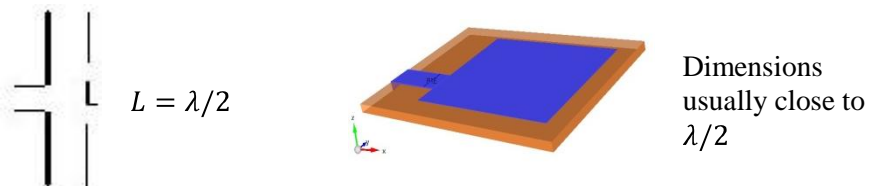


**Fig 3.6** Examples of resonant antennas: half wave dipole (left) and patch (right.)

These antennas generally have relatively low gain and narrow bandwidth. These category of antennas is one of the most commonly applied in everyday life. More discussion about these antennas are given in the subsequent chapters.

3. Broadband Antennas: spiral antennas and log periodic dipole array arrays belong to this category



**Fig 3.7** Spiral antenna as an example of broadband antenna. [61]

Broadband antennas have moderate to large gains, broad bandwidth and medium sizes.

4. Aperture Antennas: Aperture antennas are antennas that have apertures to guide the wave to radiation. Horn antennas and parabolic reflector antennas belong to these antennas.



**Fig 3.8** Examples of aperture antennas: parabolic antenna (left) and horn antenna (right) [56]

Aperture antennas have large size and big gain. The parabolic dish in reflector antennas is used to reflect the wave coming from the feed placed in front of it. Horn antennas have shapes that look like an opening wave guide guiding a wave into free space.

## 4. RECTANGULAR PATCH ANTENNA

It was mentioned in the section 3.3 that there are several antenna types. In this chapter, the discussion is narrowed to rectangular microstrip patch antennas. Microstrip antennas were first introduced in 1953 and they were manufactured first in 1970's [13]. Microstrip antennas are resonant printed antennas. They have several qualities that make them preferable to other antenna types. They are of low profile, small size, small volume, cheap, easy to manufacture and integrate to other electronics. They also have versatile frequency and polarization features.[1; 4; 9; 13]

On the contrary, Microstrip patch antennas have disadvantages that need intelligent design such as low efficiency, low power, high Q, poor polarization efficiency, poor scan performance, spurious feed radiation and very narrow bandwidths. [4]

Patch antennas are generally considered suitable for RFID readers and tags. Their low bandwidth turns out to be an advantage for RFID systems which require less bandwidth as the antenna rejects out of band signals, increasing the quality factor. [14]

One of the most common microstrip antennas are rectangular patches. The simplest form of microstrip patch antenna is as shown in figure 4.1. It is a three layer structure that has a metal patch on top with some feed, a dielectric in between and a metal ground on the bottom.

### 4.1. Analysis Techniques for Microstrip Elements

There are three widely used models to understand the principle of operation, and model microstrip antennas. Transmission line model, modal cavity model and numerical methods used in simulation softwares. Patches can come in different shapes. Here, rectangular patch is used as a reference in the models.

#### 4.1.1. Transmission Line Model

Transmission line model is the simplest model that uses transmission line theory to analyze a rectangular patch antenna. In this model the antenna is modeled as two radiating slots connected by a transmission line. As shown in the figure 4.1, each radiating edge of length  $a$  is modeled as a narrow slot radiating into a half space.

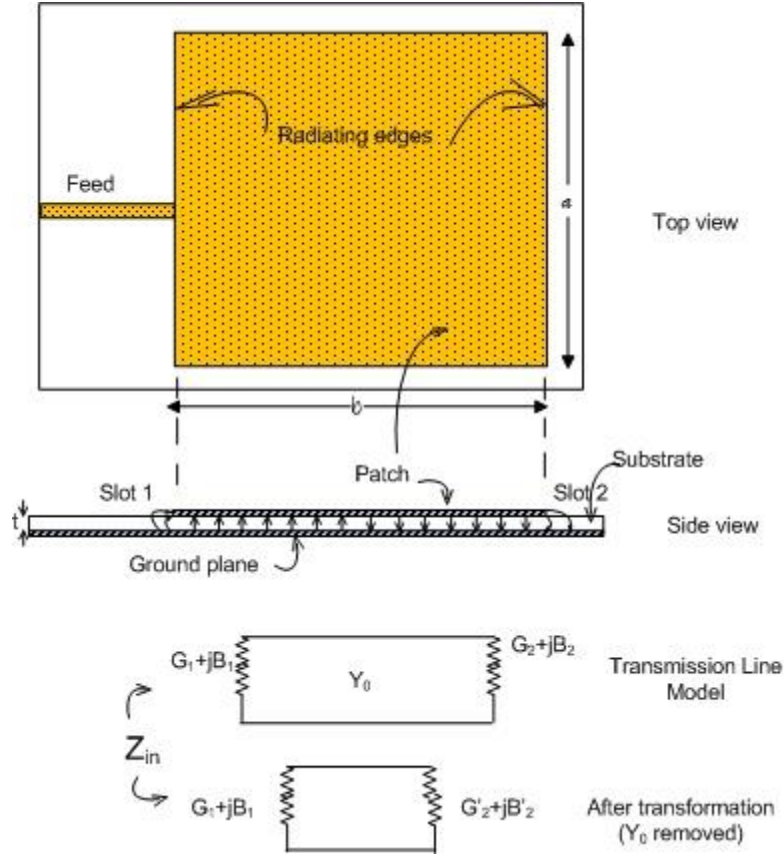


**Fig. 4.1** Transmission Line Model of Microstrip Antenna

The admittance of either of the slots is given as,

$$G_1 + jB_1 = \frac{\pi a}{\lambda_0 z_0} [1 + j(1 - 0.635 \ln k_0 w)] \quad (4.1)$$

Where  $\lambda_0$  is the free space wavelength  $z_0$  is wave impedance,  $z_0 = \sqrt{\frac{\mu_0}{\epsilon_0}}$ .  $k_0$  is wave number,  $k_0 = \frac{2\pi}{\lambda_0}$  and  $w$  is the slot width approximately equal to the substrate thickness,  $t$ . The slots are identical except for the fringing fields at associated with the feeding point at edge 1, so we can use this symmetry to calculate the admittance. Transmission line model assumes no field variation in the direction parallel to the radiating edges, so, the section between the two slots is considered as a parallel plate transmission line. Therefore, the characteristic admittance can be given as, [15]

$$Y_0 = \frac{a\sqrt{\epsilon_r}}{tz_0} \quad (4.2)$$

$t$  is the substrate thickness and  $\epsilon_r$  is relative permittivity of the substrate.

It is desired to excite the slots  $180^\circ$  out of phase to have resonance. As a result,  $b$  has to be as long as  $\frac{\lambda_d}{2}$  where  $\lambda_d$  is wavelength in the dielectric,  $\lambda_d = \frac{\lambda_0}{\sqrt{\epsilon_r}}$ . In

reality, the resonant length is reduced slightly because of the fringing fields at the radiating edges. Usually  $b \cong 0.48\lambda_d$ . [4]

With  $180^\circ$  electrical distance between the slots, after transformation, the admittance of the second slot will be,

$$\overline{G}_2 + j\overline{B}_2 = G_1 - jB_1 \quad (4.3)$$

Therefore, the total input admittance will be,

$$Y_{in} = G_1 - jB_1 + \overline{G}_2 + j\overline{B}_2 = 2G_1 \quad (4.4)$$

From equation 4.1, we can see that the length of the radiating edge ( $a$ ) affects the slot conductance. For a typical design where  $a = \lambda_0/2$ ,  $R_{in} = 120 \Omega$ . This is the resonant input impedance of a square patch antenna with microstrip feed as shown in fig. 4.1.

It should be noted that the resonant input admittance given above does not take into account the mutual effects (transadmittance) between the slots. As a direct implication from the choice of  $b$ , the resonance frequency can be calculated as [9; 14]

$$f_r = \frac{c}{\lambda_d \sqrt{\epsilon_r}} = q \frac{c}{2b\sqrt{\epsilon_r}} \quad (4.5)$$

where,  $q$  is the fringe factor that determines the resonance length reduction. It should be measured for a given substrate, then the same value can be used for different patch sizes in the same frequency range. [9]

#### 4.1.2. Modal Cavity Model

Modal cavity model considers the patch antenna as a 3D structure so it considers field variations across the radiating edge. In this model, the patch is considered as a thin  $TM_x$  mode dielectric loaded cavity with magnetic walls [9]

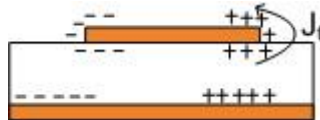


**Fig. 4.2** Charge distribution and corresponding current distribution of a patch antenna

When a patch is energized, charges will be distributed as shown in fig 4.2. Then the attractive and repulsive forces between charges create two currents. The first current is  $J_t$ , which stands for the current created by the attraction of opposite

charges on the patch surface, which also acts to balance charge distribution on the patch surface. The second current is  $J_b$ . It is the result of the attraction or repulsion of charges on the ground plane. [4; 9]

Normally, patch antennas have thickness very small thickness compared to their length and width, i.e.  $h \ll L, W$ . This creates a scenario where by most of the charge motion is controlled by the  $J_b$ . This leads to the assumption that,  $J_s = 0$  which in turn implies that the tangential magnetic fields are zero at the walls of the patch. Consequently, as the first assumption, the patch is approximated as a cavity with magnetic side walls. [4; 9]

As a second assumption, the dielectric is assumed to be covered by perfect electric conductor (PEC) on top (the ground) and bottom (the patch). Therefore, the electric field is normal to the patch surface. [4; 9]

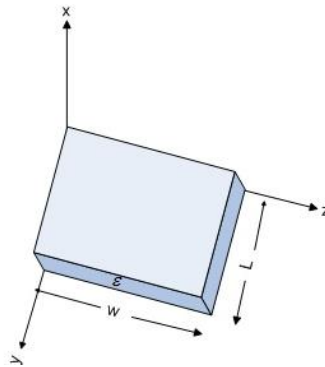


*Fig. 4.3 modeling patch as cavity*

However, treating microstrip antenna only as a cavity is not sufficient to find the absolute amplitudes of the electric and magnetic fields. Besides, treating the walls of the cavity, as well as the material within it as lossless, the cavity would not radiate and its input impedance would be purely reactive just like usual cavity resonators. The model accounts for radiative loss by introducing effective loss tangent.  $\delta_{eff} = \frac{1}{Q}$ . The waves generated within the microstrip undergo considerable reflections when they arrive at the edge of the patch because thickness of the microstrip is usually very small. Therefore, only a fraction of energy is radiated which accounts for the low efficiency of microstrip patch antennas. [1]

Now, the fields beneath the patch form standing waves that can be represented by cosinusoidal wave functions. The field variations along  $h$  (as in the fig. 3.2 above) (the same choice of axis as shown in the picture is used in the whole thesis) remain constant accounting for small  $h$ . The fringing fields tend to be zero and the electric field tends to be normal to the patch at the edges. Therefore, only  $TM_x$  fields are considered in the cavity. [4]

The field configurations within the cavity can be calculated according to equation 2.4. To drive the field configurations that are TM to a given direction, it is

sufficient to let  $\mathbf{A}$  have a component in the direction in which the fields are desired to be TM, in our case, the x-axis. [3]

$$\nabla^2 A_x + k^2 A_x = 0 \quad (4.6)$$

Using the separation of variables, the solution is written in general as, [4]

$$A_x = [A_1 \cos(k_x x) + B_1 \sin(k_x x)][A_2 \cos(k_y y) + B_2 \sin(k_y y)][A_3 \cos(k_z z) + B_3 \sin(k_z z)] \quad (4.7)$$

where,  $k_x$ ,  $k_y$ ,  $k_z$  are wave numbers along  $x$ ,  $y$  and  $z$  directions respectively which are determined subject to the boundary conditions. Then we can calculate the field values,  $\mathbf{E}$ , and  $\mathbf{H}$  using the relations in Maxwell's equations.

$$E_x = -j \frac{1}{\mu\omega\epsilon} \left( \frac{\partial^2}{\partial x^2} + k^2 \right) A_x \quad H_x = 0 \quad (4.8)$$

$$E_y = -j \frac{1}{\mu\omega\epsilon} \frac{\partial^2 A_x}{\partial x \partial y} \quad H_y = \frac{1}{\mu} \frac{\partial A_x}{\partial z} \quad (4.9)$$

$$E_z = -j \frac{1}{\mu\omega\epsilon} \frac{\partial^2 A_x}{\partial x \partial z} \quad H_z = \frac{1}{\mu} \frac{\partial A_x}{\partial y} \quad (4.10)$$

The cavity has been assumed as four perfectly conducting magnetic walls and two perfectly conducting electric walls at the top and bottom. Therefore, we can solve for  $A_x$  using these boundary conditions.

$$k_x = \frac{m\pi}{h}, \quad m = 0, 1, 2, \dots \quad (4.11)$$

$$k_y = \frac{n\pi}{L}, \quad n = 0, 1, 2, \dots \quad (4.12)$$

$$k_z = \frac{p\pi}{W}, \quad p = 0, 1, 2, \dots \quad (4.13)$$

With  $B_1 = B_2 = B_3 = 0$ , and  $A_{mnp} = A_1 A_2 A_3$ ,  $A_x$  can be rewritten as,

$$A_x = A_{mnp} \cos(k_x x) A_2 \cos(k_y y) A_3 \cos(k_z z) \quad (4.14)$$

$m, n,$  and  $p$  represent the number of half cycle field variations along the  $x, y$  and  $z$  directions respectively.

The wave numbers  $k_x, k_y,$  and  $k_z$  are subject to the constraint equation [4]. The constraint equation is an indication that the resultant wave travels at the speed of light altogether.

$$k_x^2 + k_y^2 + k_z^2 = \left(\frac{m\pi}{h}\right)^2 + \left(\frac{n\pi}{L}\right)^2 + \left(\frac{p\pi}{W}\right)^2 = k_r^2 = \omega_r^2 \mu \epsilon \quad (4.15)$$

As a result, the resonant frequencies for the cavity are then given as,

$$f_{r,mnp} = \frac{1}{2\pi\sqrt{\mu\epsilon}} \sqrt{\left(\frac{m\pi}{h}\right)^2 + \left(\frac{n\pi}{L}\right)^2 + \left(\frac{p\pi}{W}\right)^2} \quad (4.16)$$

The field values can then be found out by replacing equation 3.6 in the field values. Therefore, unlike the transmission line model, resonance happens at more than a single frequency. Placing the resonant frequencies in ascending order determines the order of the modes of operation. Practically, in Microstrip antennas  $h \ll L$  and  $h \ll W$ . If  $L > W > h$ , the mode with the lowest frequency (dominant mode) is the  $TM_{010}^x$  whose resonant frequency is given by, [4]

$$(f_r)_{010} = \frac{1}{2L\sqrt{\mu\epsilon}} \quad (4.17)$$

whereas, if  $W > L > h$ , then the dominant mode will be  $TM_{001}^x$  and the resonant frequency is given as,

$$(f_r)_{001} = \frac{1}{2W\sqrt{\mu\epsilon}} \quad (4.18)$$

We could have other modes if the length is more than twice the width or vice versa. However, it is rather practical to just consider shapes closer to a square.

So far, we have ignored the fringing effects along the edges of the cavity. We have seen in transmission line model earlier that there is a shift in oscillation frequency as a result of the fringing effects. The same assumption follows for the cavity model.

For instance for the dominant  $TM_{010}^x$  mode the resonance frequency will be

$$(f_r)_{010} = \frac{q}{2L\sqrt{\mu\epsilon}} \quad (4.19)$$

We have assumed that the cavities do not extend beyond the edges of the patch. So, the four sidewalls represent four narrow apertures through which radiation takes place. [4]

Huygen's field equivalent principle says actual sources, such as antennas, are replaced by equivalent fictitious sources that produce the same fields within the region. Accordingly, the microstrip patch is represented by an equivalent electric current density  $J_t$  at the top surface of the patch to account for the presence of the patch. Then the four side walls are represented by the equivalent electric current density,  $J_s$  and equivalent magnetic current density,  $M_s$ . These currents are given as, [4; 6]

$$J_s = \hat{n} \times H_a \quad (4.20)$$

$$M_s = -\hat{n} \times E_a \quad (4.21)$$

It was assumed that,  $J_s = 0$  So we can ignore the effect of  $H_a$ . The only non zero current left is the equivalent magnetic current density,  $M_s$ . According to image theory, the presence of the ground plane doubles the equivalent magnetic current density. Consequently, [4; 6]

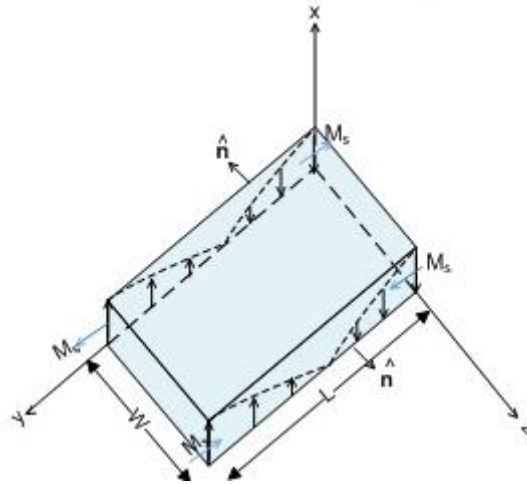


**Fig. 4.4** Current distribution in  $TM_{010}^x$  mode

$$M_s = -2\hat{n} \times E_a \quad (4.22)$$

While there are four slots with this current, only two of them, known as radiating slots, account for the radiation. This is because the fields created by the other two slots cancel. This is in agreement with transmission line model where only the edges along the length of the patch radiate.

The radiating slots are separated by a half wave length low impedance parallel plate transmission line which acts as a transformer. The  $\lambda/2$  separation is so that the apertures of the two slots will have opposite polarizations. [4]

Let us assume the dominant mode of  $TM_{010}^x$  for the rest of the discussion of the equivalent current densities and radiations. The electric and magnetic field components substituting the wave numbers and  $A_x$  for  $TM_{010}^x$  will be,

$$E_x = E_0 \cos\left(\frac{\pi}{L}y'\right) \quad (4.23)$$

$$H_z = H_0 \sin\left(\frac{\pi}{L}y'\right) \quad (4.24)$$

$$E_y = 0, E_z = 0, H_x = 0, H_y = 0 \quad (4.25)$$

where,  $E_0 = -j\omega A_{010}$  and  $H_0 = (\pi/\mu L)A_{010}$ .

From equations 4.23-4-25, the electric field for  $TM_{010}$  will be constant along the width and will have a phase reversal along the length (y-axis). We have said that each slot radiates with a current density  $\mathbf{M}_s$ , as given in 4.22. Accordingly, referring to the figure, the slots on the left and right have magnetic currents of the same magnitude and phase. These two sources will add in a direction normal to the patch and ground plane forming a broadside pattern.

Meanwhile, again following 4.22, for the magnetic current densities on the other two slots (front and back), since the current densities on each wall are of the same magnitude but opposite direction, the fields radiated by these two slots cancel each other in the principal H plane. In addition, the fact that the currents on the slots are in opposite direction, leads to a cancelation in the principal H plane. [4]

### 4.1.3. Computational Models Used by Simulation Software

Analytical models have been discussed so far. But these methods represent only the basic shapes and more complicated as more complicated structures are used. Therefore, several computational models have been proposed to overcome this limitation.

CST Microwave Studio (CST MWS) [16] and Empire XCcel [17] were the two simulation softwares used for the project. CST MWS uses finite integration technique (FIT) where as Empire XCcel is based on finite difference time domain (FDTD) technique. FIT and FDTD are two common algorithms used to solve electromagnetic waves on given material and geometrical specification for the given boundary conditions.

FDTD is a method that finds the solution to Maxwell's curl equations. In FDTD the illumination of a structure is the initial-value problem. At time,  $t = 0$ , a plane-wave source of frequency  $f$  is assumed to be excited Then FDTD simulator simulates the propagation of waves from this source by solving a finite-difference

analog of the time-dependent Maxwell's equations on a lattice of cells, including the structure. Time-stepping is continued until the sinusoidal steady state is achieved at each cell. The field envelope, or maximum absolute value, during the final half-wave cycle of time-stepping is taken as the magnitude of the phasor of the steady-state field at each cell. [18]

Time stepping for the E field can be done in such a way that the change in electric field in time is (time derivative) equals the spatial derivative (curl) of the H field. This establishes the first FDTD relation in which at any point in the space, the updated value of the E field in time is dependent on the stored value of the E field and the numerical curl of the local H field. Similarly the second FDTD relation, the H field is updated from the stored H field and the numerical curl of the local distribution of the E field. [18]

On the other hand FIT is a numerical method that discretises the integral forms of Maxwell's equations. To solve these equations numerically, a finite calculation domain is defined, enclosing the considered application problem. Creating a suitable mesh system splits this domain up into many small elements, or grid cells. A primary mesh can be seen in the mesh view of the software but, in addition to this, the second mesh is established orthogonal to this. These orthogonal meshes define the spatial discretization for the equations. The fields are then systematically oriented in the facets and edges of the meshes. Finally, the solver equates the matrices that come from the numerical field relations. [16]

## 4.2. Characteristics of Rectangular Patch Antennas

Basic characteristics rectangular patch antennas is discussed next. These main characteristics include radiation fields, bandwidth, directivity, gain and feeding techniques.

### 4.2.1. Radiation Fields of Rectangular Patch Antennas

Generally the radiation fields decay as we go away from the antenna with  $\frac{1}{r^2}$ , r being the separation, but the variation in angle at a fixed distance ( $\theta, \phi$ ) depends on the antenna. Far field radiation patterns demonstrate this angular behavior of an antenna as the separation goes to infinity.

The coordinate system in fig. 3.1 and a patch antenna oriented on the xy plane is considered. Taking the spherical coordinates, the total far field electric fields radiated by the patch can be obtained with modal cavity model. [4; 13]

The mode  $TM_{010}^x$  is activated when the feed is given from y-axis. Accordingly, we see that in the principal E plane  $E_\theta$  dominates and  $E_\phi$  will be comparatively very small and sometimes considered as a cross polar component. On the contrary, in the

principal H plane  $E_\phi$  dominates and  $E_\theta$  is small in comparison and is considered the cross polar component. [4; 13]

#### 4.2.2. Bandwidth of Rectangular Patch Antennas

The usual definition of bandwidth was given earlier. A more relevant definition is given, the impedance or VSWR bandwidth of an MSA is the range of frequency in which the antenna is matched to the feed within specified VSWR limits. It is also inversely proportional to the quality factor, Q. [13]

Mathematically,

$$BW = \frac{VSWR - 1}{Q\sqrt{VSWR}} \quad (4.26)$$

VSWR refers to Voltage Standing Wave Ratio and is defined with the input reflection coefficient as

$$VSWR = \frac{1 + |\Gamma|}{1 - |\Gamma|} \quad (4.27)$$

Where,  $\Gamma$  is defined as

$$\Gamma = \frac{Z_{in} - Z_0}{Z_{in} + Z_0} \quad (4.28)$$

where  $Z_{in}$  and  $Z_0$  are the input impedance of the antenna and the feed respectively. Now we can see,  $|\Gamma| \leq 1$  and  $VSWR \geq 1$ .  $VSWR = 1$  implies a perfect match, where as  $VSWR = \infty$  implies a total reflection. In the equation we use the linear value but the figure can also be given in dB. [2; 4]

MSA bandwidth is usually specified for  $VSWR < 2$ , which accounts for 9.5 dB return loss. Sometimes the figure is 1.5 for strict applications and that accounts for a return loss of 14 dB. [13] The BW of a single-patch antenna increases with an increase in the substrate thickness and decreases with the square root of the  $\epsilon_r$  of the substrate. [19; 20]

Practically several techniques can be implemented to enhance the bandwidth of MSAs. For RMSAs (Regularly shaped MSAs) such as the one shown in fig.1 simply increasing the width ( $b$  in this case) increases the bandwidth, with other parameters fixed. [13]

Common methods of enhancing MSA bandwidths have been suggested in several works generally include. One of these methods is using thicker substrates. Using planar gap coupled or direct coupled multiresonators also advances bandwidth in expense of size. Broadband matching techniques such as stubs and coplanar

waveguides have also been used for the same purpose. In addition, altering patch width also increases bandwidth. Choice of substrate has an effect on bandwidth. Substrates with smaller dielectric constant bear larger bandwidth. In aperture antennas using resonant apertures with resonance of close proximity with the patch in aperture fed antennas. [1; 13]

Most of these methods however vary from design to design. In addition advancing the bandwidth may also have compromises. For instance, lowering dielectric constant makes the antenna bigger; increasing thickness in probe fed antennas increases inductive reactance of the probe. Therefore, these parameters need to be tuned with respect to specific model.

### 4.2.3. Directivity and Gain of Rectangular Patch Antennas

The maximum directivity of the radiating slots of microstrip antenna approximately equals [4]

$$D_0 = \begin{cases} 6.6 \text{ (linear)} = 8.2 \text{ dB}, W \ll \lambda_0 \\ 8 \left(\frac{W}{\lambda_0}\right), W \gg \lambda_0 \end{cases} \quad (4.29)$$

The directivity of a rectangular shaped MSA can be calculated approximately as, [13]

$$D = 0.2W + 6.6 + 10 \log \left( \frac{1.6}{\sqrt{\epsilon_r}} \right) \text{ dB} \quad (4.30)$$

MSA gain, like any antenna gain, is calculated by subtracting the logarithmic efficiency from the logarithmic directivity. It has been mentioned in modal cavity model that MSAs have very low efficiency as most of the waves get reflected. Generally efficiency can be improved by using substrates with low loss tangent and low dielectric constant. Still, as it was the case for bandwidth, design parameters need to be optimized for gain for the specific design/model in mind. [4; 19; 13]

### 4.3. MSA Feed Techniques

So far, it has not been paid attention to the element that excites the antenna. Antenna feed line is a transmission line connecting the antenna with the rest of the transceiver circuit. Basically, MSAs can be fed by microstrip lines, coaxial probe and slot. These basic feed mechanisms can be modified or combined to come up with other feeding techniques. [7]

One option for microstrip line feeds is making the radiating patch a continuation of the microstrip line. On the other hand, the microstrip feed may serve as an open stub in a different layer coupling to the patch electromagnetically. Aperture and proximity coupling are examples for this.

Novel feed techniques can be created with different combinations of the above two depending on the design goal. Different feeding techniques that fit dual polarized antennas are indicated in section 6.2.

## 5. OVERVIEW OF RFID SYSTEMS

This chapter first discusses RFID as an automatic identification system. Then different RFID types and parts are discussed. Finally, reader antennas for fixed objects are discussed.

### 5.1. RFID as an Automatic Identification System

Currently, automatic identification (AutoID) is extensively used in many areas in our daily life such as purchasing and distribution logistics, manufacturing companies and material flow systems. These Auto ID systems provide information about goods, animals or even people. Common standard identification systems include barcode system, optical character recognition, biometric identification: fingerprint procedure, voice identification, smart cards and RFID. [21]

Among these AutoID systems, bar code labels, that triggered a revolution of identification systems, now face some challenges such as low data density and lack of programmability. A more sound system to resolve this would be to replace them with smart cards but they also cause difficulty because smart cards need mechanical contact. [10; 21]

There are several qualities that make RFID a preferable identification method in comparison with other identification methods. RFID systems have very high data density. Machine readability is also good in RFID systems. They also have better security features as they cannot be interrupted by people and cannot be copied by unauthorized body. This feature is revealed by authentication protocols used and the fact that RFID tags cannot be forged like magnetic systems, etc. Their other good quality is good environmental characteristics, such as no degradation or wear. One of the best qualities of RFID systems is very good tag mobility with read ranges up to several meters more than other the available systems. Besides, reading speed is also good and normally takes less than 0.5 seconds.

### 5.2. Classification of an RFID System

A generic RFID system is made up of two components: a transponder or tag that is placed on the object to be identified and a reader or interrogator.

Based on the inclusion of a battery and transmitter in their tags, RFID systems can be divided in three – active, semi passive and passive RFID systems. Active RFID systems have tags that have a battery. Passive tags do not have an independent power source and transmitter of their own. Passive RFID tags are made from passive

components, such as diode and capacitor, that rectify the electromagnetic energy coming from the reader. Semi passive RFID systems are battery assisted passive systems. Like passive tags the tag to reader communication is carried away by the rectified power; however, semi passive tags have batteries to assist the tag circuitry. [19; 21]

Passive tags have no battery which means they have long life. Besides, passive tags have no transceiver circuitry such as crystal frequency reference, synthesizer, power amplifier and LNA (Low Noise Amplifier). The elimination of such components reduces the cost and size of tags. These reasons have made passive RFID preferable active and semi active RFID systems. [19; 21]

The question of which frequency to use should be raised at this point. RFID systems use frequencies that differ by a factor of 20,000 or more from 100 KHz up to 5 GHz. Most commonly implemented bandwidths are [10]

- 125/134 kHz (LF Low Frequency band),
- 13.56 MHz , HF (High Frequency) band and
- 860–960 MHz and 2.4–2.45 GHz which are UHF (Ultra High Frequency) band

When the wavelength is much larger than dimensions of the antenna, almost all the radiated energy is located near the antenna. The communication can happen in such a way that the change in the tag induces a change in the impedance of the reader. Here the tag-reader systems act as a “magnetic transformer” coupling between the current in the reader and the voltage in the tag. Such coupling is called inductive coupling. Because of their big wavelength, LF systems have inductive coupling. On the contrary, when the antenna size is comparable with the wavelength, we can talk about separate transmitted and reflected waves and such coupling for higher frequencies is called radiative coupling. [19; 21]

Inductive coupling falls fast as the tag moves away from the reader. As a result, the read range of inductively coupled antenna is comparable to the size of the reader antenna. Besides, inductive coupling uses coils instead of tags which are handy. Meanwhile radiative coupling could be possible to even several meters and as the frequency gets bigger, the size of the tag antennas gets smaller, which makes 2.4-2.5 GHz systems the best as far as low size, flexibility and cost considered. But 2.4 GHz based tags collect less power for the given radiated power as compared to 860–960 MHz based tags which will make them have less read range. So UHF tags have wide spread use in comparison to others in areas such as automobile tolling, supply chain management, transport baggage tracking, and asset tracking. This thesis discusses reader antennas proposed for passive UHF RFID systems. [10; 21]

### 5.3. Applications of RFID Systems

Biometric or e-passports are becoming common in many parts of the world. A chip and an antenna are embedded in a passport making biometric identification possible. The chip is used to contain and communicate information such as the subject's face, fingerprint, and basic information such as birth date. The fact that RFID tags can neither be counterfeited nor eavesdropped has created considerable confidence in implementing them in such applications that demand strong security. [10; 21]

The other application is asset tracking. The assets can be company properties or personal belongings such as electronic devices, keys, wallet or passport. The application can then be used with a network of readers. Once the location of the reader is known (with the help of GPS or other means), then the asset(s) can be tracked or retrieved if lost. [10; 21]

There are yet many applications to mention such as Point of Sale (POS), Automated Vehicle Identification (AVI) systems, Asset tracking, Pet ownership identification, Warehouse managements and logistics, Product Security, Library books check-in/check-out. [10; 21; 22]

### 5.4. UHF RFID Systems

As mentioned above in passive RFID communication, the tag doesn't have its own power. Instead, it uses the rectified RF power from the reader. For the backscattering to work, the tag antenna has to effectively radiate back. Fig. 5.2 below shows generic UHF RFID system.

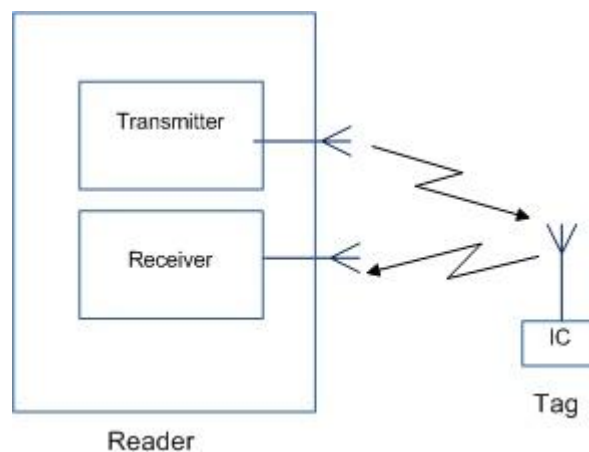


*Fig. 5.1 A generic UHF RFID system with reader*

Internationally, every there are different UHF RFID standards in different parts of the world. Table 5.1 summarizes bands allocated for different locations.

**Table 5.1** UHF RFID Allocated bands and maximum transmission power. [10]

Country/region (standard)	Allocated frequency (MHz)	Maximum Tx. Power (W)
Europe	865-868	0.5
USA	902-928	2.4
Korea	908.5-914	2.4
Japan	952-954	2.4
China	840.25-844.75	2.0
China	920.25-924.75	2.0
Brazil	902-907.5	2.4
Brazil	915-928	2.4
South Africa	865.6-867.6	2.0
South Africa	917-921	2.4

UHF RFID readers are transceivers that transmit and receive at the same time. For efficient communication, there has to be good isolation between transmit and receive channels, to easily decode and detect the weak backscattered signals coming from the tags [23]. Therefore, as long as the design of the antenna is concerned, the bandwidth should be wide enough to provide the two channels.

## 5.5. Link Budget for a UHF RFID System

In passive RFID communication the small signal received by the antenna is divided between power given to the IC and power radiated back to the reader. So, the power has to be efficiently managed to be able to radiate back and to keep the IC working.

In the first place, the reader sends symbols coded to ensure that sufficient power is always transmitted irrespective of the data contained in it. The tag antenna detects that and with the control of its load impedance state, it radiates back. [10]

It is thus crucial to know the power level required by the tag to operate to know how far it can be away from the reader. The amount of power a receiver needs to successfully interpret the data is called link budget. In two way communications like RFID systems, we will have forward link (reader to tag) and reverse link budget (tag-to reader). Due to license regulations the reader cannot transmit more than 1 W (30 dBm).

Before discussing the tag power requirement for efficient communication, path is defined. Path Loss is the difference between power delivered to the transmit antenna and power obtained from the receiver antenna. For an isotropic antenna the received power  $P_{RX}$  is [24]

$$P_{RX} = P_{TX} \frac{A_e}{4\pi r^2} \quad (5.1)$$

$P_{TX}$  is transmitted power and where  $A_e$  is the aperture area, for an isotropic antenna,

$$A_e = \frac{\lambda^2}{4\pi} \quad (5.2)$$

For instance, for transmitted power of 30dBm=1 W, after 1m with this formula, we get 0.7 mW =-1.6 dBm. This stands for a path loss of 30 dBm-(-1.6 dBm) = 31.6 dBm.

Forward link budget stands for the minimum power required for reader to tag communication. Modern tag ICs actually consume around 10 – 30μW to operate (much power is required to write new data to the tag memory). The rectifying circuit is only 30% efficient. As a result, about 30-100 μW is required. With 100 μW = –10 dBm received power level, we will have 40 dBm path losses which is a distance of 3m according to the formula above. [10]

Reverse link budget stands for the minimum tag to reader communication. Theoretically, it is possible for the tag to backscatter up to four times as much power as it could absorb- but if it does so, the IC will receive no power at all. Actual modification varies from design to design. A reasonable estimate for our purposes is to assume a modulated backscatter power around 1/3<sup>rd</sup> of the absorbed power. A convenient plausible lower limit of around -75 dBm (0.03 nW). If we consider the same 3m separation, the tag has to transmit around -55 dBm. This figure is 20 dB less the power the tag can send. So we can see that *RFID communication is forward link limited*. The reason being that the IC needs more much more power as compared to the small signal needed to be detected by a good quality low sensitivity reader. [10]

In the reverse link, the received energy depends on the effective aperture or area. Intuitively and from the principle of reciprocity the size of the receiving aperture is proportional to the gain of the antenna when it is used as a transmitter. [10; 24]

$$A_e = G \left( \frac{\lambda^2}{4\pi} \right) \quad (5.3)$$

This leads to the famous Friis' formula for finding the received power, [24]

$$P_{RX} = P_{TX} G_{TX} G_{RX} \left( \frac{\lambda}{4\pi r} \right)^2 \quad (5.4)$$

We can modify the Friis' equation for RFID. We define the gain of the tag antenna  $G_{tag}$  and *backscatter transmission loss*  $T_b = 1/3$ . [10]

$$P_{TX,tag} = P_{TX,reader} G_{reader} G_{tag} \left( \frac{\lambda}{4\pi r} \right)^2 T_b \quad (5.5)$$

$$P_{RX,reader} = P_{TX,tag} G_{tag} G_{reader} \left(\frac{\lambda}{4\pi r}\right)^2 T_b \quad (5.6)$$

Combining the two equations above, we have,

$$P_{RX,reader} = P_{TX,reader} (G_{reader})^2 (G_{tag})^2 \left(\frac{\lambda}{4\pi r}\right)^4 T_b \quad (5.7)$$

Replacing this equation in 4.1 and evaluating, we can then define the read ranges for forward and reverse links. [11]

$$R_{forward} = \left(\frac{\lambda}{4\pi r}\right) \sqrt{\frac{P_{TX} G_{reader} G_{tag}}{P_{min,tag}}} \quad (5.8)$$

$$R_{forward} = \left(\frac{\lambda}{4\pi r}\right)^4 \sqrt{\frac{P_{TX,reader} T_b G_{reader}^2 G_{tag}^2}{P_{min,rdr}}} \quad (5.9)$$

The read range analysis here does not take into account polarization state. Polarization as well affects read range. For instance, a circularly polarized wave can interact with a linear antenna tilted at any angle perpendicular to the plane of propagation but only half the transmitted power can be received. More about this is mentioned later in chapter 6.

A modest improvement in this situation results when physically larger ‘bow-tie’ like antenna designs are used since electric fields at small angles to the axis of the antenna can still induce current flow.

## 5.6. Review of Reader Antennas

The readers antennas considered here are antennas for fixed readers. Other common RFID reader antennas include reader antennas for hand held and portable readers and near field antennas.

RFID reader antennas currently available can be characterized in their datasheets by [10]

- Gain (maximum gain): The gain values for most RFID reader antennas range 5-10 dBi but standards and interference in multi-antenna systems limit gain.
- Radiation Pattern: also gives information about beam width.
- Bandwidth: it can be European, US ISM band, wideband for all RFID bands, etc.

- Polarization: the antenna can be linear, circular or dual polarized and
- Mechanical parameters

Passive RFID readers can monitor the flow of goods through some checkpoint such as door, portal or gateway. They can also be used in conveyers. Directional antennas are preferred for such applications. However the beam width should also be kept to keep the needed read area. The bandwidth choice depends on the standards and location. The other matter that passive RFID readers differ is in their polarization. Further discussion with regards to polarization of readers is discussed in the next chapter.

In the next section survey of fixed reader antennas is done. Patch antenna is the very common RFID reader antenna [10]. Depending on the application needed, the parameters mentioned above are optimized by tuning patch structure, size, composition, etc.

The main problem patch antennas have is very narrow bandwidth; however, RFID applications do not generally need big bandwidth. This can be an as the antenna rejects out of band signals its quality factor increases. [25]

### 5.6.1. Structure and Feed

Feeding techniques are closely related with the structure of antennas. RFID reader antennas so far follow different structures and feeding techniques. Some of these are as simple as planar single layer inset feed [25] or more complicated novel designs with multiple layers [26; 27: 28]

Aperture coupling is one of the common feed types. Such feeds are preferred for instance when less spurious feed radiation is needed as the feed is isolated from the patch by the ground plane. Besides, the bandwidth can be expanded by optimizing the coupling effect between the patch and the aperture [29] In addition aperture coupling helps for good isolation between different ports by following different aperture position and shapes. For instance in [30] rotating the cross shaped aperture produces improved isolation.

Sometimes a single microstrip line could be coupled in aperture such as in [31] for single feeds. In two feed/port antennas, usually the (example) two microstrip lines are spatially orthogonal and serve for generating dual or circular polarization. [30; 32] Other feed type implemented in RFID reader antennas is probe feeding. [33] These designs grant compact designs and hide the feed behind the ground plane [1].

In addition to these, some antennas follow novel feeding techniques. For instance [34] has a patch fed by four probes which are sequentially connected to the suspended microstrip feed line, or [23] has single L shaped ground coupled metal sheet as a feed element. This project proposes the possibility of proximity coupling to reader antenna.

### 5.6.2. Polarization

Linear polarization is the simple polarization by some of the RFID readers proposed so far [30]. To reduce the polarization mismatch caused by tags circularly polarized antennas have been proposed in different IEEE papers. There have been also some dual polarized antennas. More is discussed about polarization in the next chapter.

### 5.6.3. Bandwidth

Reader antennas can be designed to have all or part of frequency bands from the global RFID band. There have been design of antennas for US band [23], Japanese band [35] or European band [25]. Broadband antennas have also been implemented that cover the entire band. For instance [27] is designed to have a -10 dB return loss and 3 dB axial ratio in the entire RFID band. Besides, there are also some dual band antennas that operate in more than one standard. For instance [36] has been reported to have an impedance bandwidth for 1:2 VSWR of 16.7% at UHF band (880 MHz-1.04 GHz) and 31% at microwave band (1.96GHz-2.68 GHz).

Several peculiar techniques have been included in designs to improve bandwidth. Generally a broadband antenna is flexible and allows interoperability between devices. We have seen that the techniques to make broadband either require larger size [13] , [34] or modification the basic RMSA structure by optimizing the existing parameters , or inclusion of additional structures ( for instance [37] adds additional patches and vias between layers) These options should however be considered with the manufacturing cost.

### 5.6.4. Gain

Tags have low gain antennas with limited EIRP. As a result, a high gain antenna is needed to increase the read range. However, it has been mentioned earlier in section 5.3 the gain of antennas for fixed readers is limited by standards and interference. Generally, in RFID reader antennas, the gain can be enhanced by increasing both the patch and the ground plane size [31].

There is a wide variation of gain in reader antennas. In some it is as low as -2 dBi or as large as 11.2 dBi [23]. [23] mentions the small size the reason for small gain. Like bandwidth the gain is enhanced following different novel approaches. For instance [38] uses short horns to enhance the gain of a circularly polarized patch antenna. A common method is to use a metal reflector behind the ground plane to suppress the backside radiation and enhance the directional gain. [39] [40] proposes the use of EBG (Electromagnetic Band Gap).

These are ground planes, periodic structures in which the propagation of certain bands is prohibited. to enhance the gain by improving the antenna efficiency and reduction of side lobes.

In conclusion, there are various proposals of patch antennas for fixed RFID readers that have been made to fit to the needed criteria discussed above.

## 6. DUAL POLARIZED ANTENNAS

So far, in many applications such as radars and mobile systems, dual polarized antennas have been used either where different information can be carried with the different polarizations or where there is a limited spectrum so that the bandwidth can be doubled with the utilized orthogonal polarizations [1; 13]. Both of these applications require a high degree of isolation between the orthogonal polarizations. In this project/thesis, the main purpose of using dual polarization is to reduce the polarization mismatch caused by an arbitrary orientation of tags and the input isolation is not that the main factor.

### 6.1. Polarization Loss Factor

Generally, for an incoming wave with the electric field vector,  $\mathbf{E}_i = \hat{\rho}_w E_i$  and a received wave,  $\mathbf{E}_a = \hat{\rho}_a E_a$  polarization loss factor (PLF) can be defined as [4]

$$PLF = |\hat{\rho}_w \cdot \hat{\rho}_a|^2 \quad (6.1)$$

PLF ranges from zero (complete mismatch) to unity (total match). In linear tag to linear receiver communication, PLF values can take any of these values depending on the orientation of the tag. Circularly polarized antennas have polarizations that vary constantly across a circle so the average PLF = 0.5. [4]

Dual polarization in the context of RFID systems where the tags are linear while the readers are dual polarized is tricky. The reason is because the mechanism of signal transmission is not symmetric. Figure 6.1 is used to illustrate this scenario. The reader is positioned in the  $yz$ - plane. It is dual polarized and generates orthogonal waves which sum up to produce a single linear wave that can be resolved into  $y$  and  $z$  axis. The signal reaches the tag only if the tag has a component in the direction of the linear wave. If the tag is parallel to the combined linear wave, the signal is completely received, but if the tag is perpendicular to the combined linear wave, then the signal is completely lost. Nonetheless, it is not the same when the tag is transmitting. This is because whichever way in the  $xy$  planes the tag is placed, it emits a single polarized wave and the dual polarized receiver will be able to receive the wave.

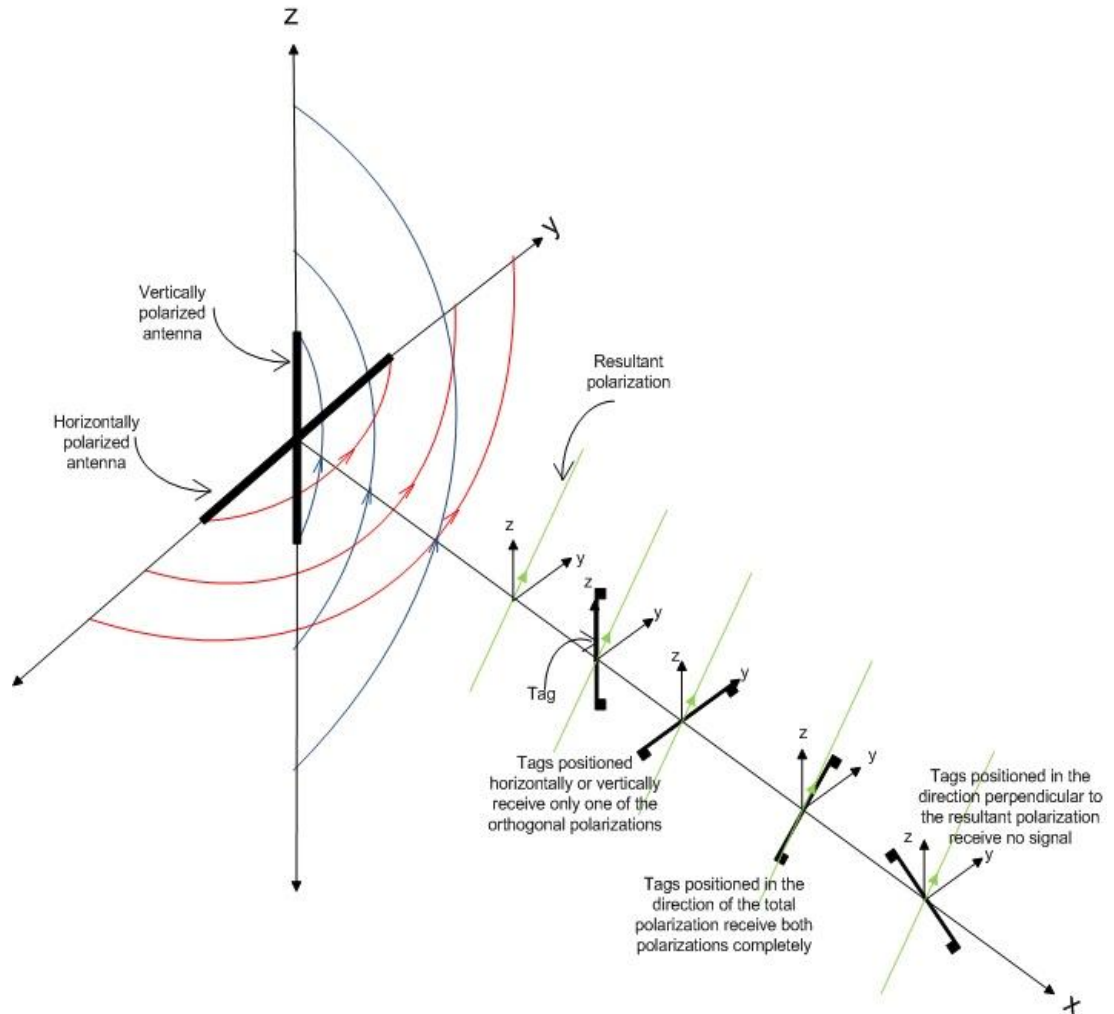


**Fig 6.1** Tags oriented in different directions with respect to a dual polarized antenna

Thus we see in their simplest form, The PLF of dual polarized antennas are superior to horizontal or vertical polarized antennas only in wave reception. However, PLF can be improved if the reader incorporates a system that can adapt to the orientation of the tag. The following figure illustrates this scenario.

As we see from figure 6.2 below, adjusting the amplitude levels of the two orthogonal inputs with in phase signals covers a tag that is positioned in the 1<sup>st</sup> and 3<sup>rd</sup> quadrant. Doing the same with the two inputs at 180 degrees out of phase does the same for a tag in the 2<sup>nd</sup> and 4<sup>th</sup> quadrant. Consequently, it can be seen that the PLF can theoretically reach up to 100%.

Consequently, we can see that dual polarized antennas with receiver features mentioned above have superior PLF as compared to linearly polarized antennas in both transmission and reception.

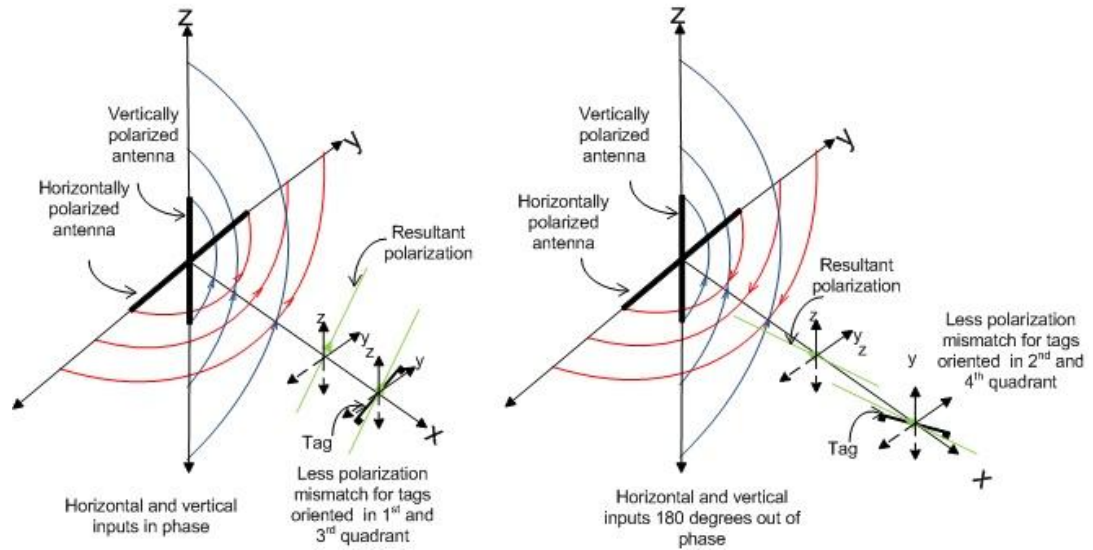


**Fig 6.2** Adjusting phase to decrease polarization mismatch

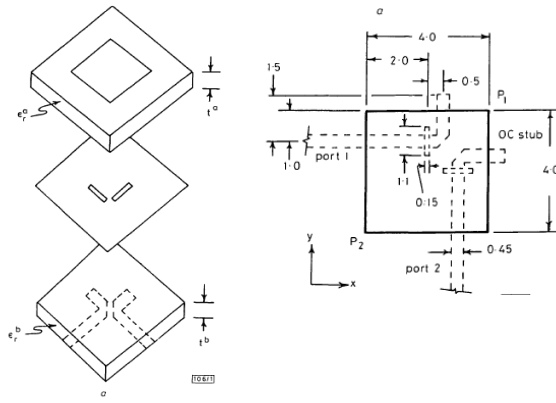
The same is true for circularly polarized antennas. Both the forward and reverse communication of a circularly polarized antenna have PLF of 0.5. So we see using dual polarized receiver automatically improves the reverse communication. On the other hand, the forward communication features of dual polarized antenna with the reader that actively adapts to the tag antenna orientation are superior to circularly polarized antennas.

## 6.2. Main Design Considerations of Dual Polarized UHF RFID Patch Antennas

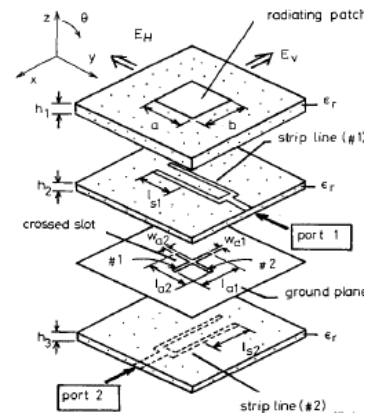
Dual polarized antennas have more design challenges than single polarized antennas. In the next section design considerations such as designing the feeds, isolation bandwidth and gain are discussed. Comparison of some of the key parameters of dual polarized antennas for some selected papers is shown in appendix 1.

### 6.2.1. Designing the Feeds

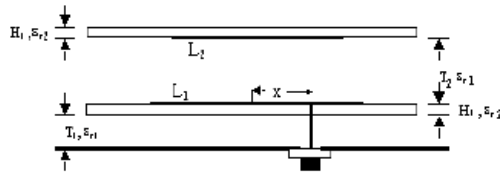
The feeds can be designed considering separate patches for each input as is given in fig 6.3 d) [41]. On the contrary, compact dual polarized antenna designs call for using two orthogonal modes in a single patch. The compact antennas can be fed by two different coaxial feeds, microstrip or strip lines. More compact designs can be done using a single coaxial feed, microstrip or strip lines with power splitting network such as hybrid coupler. The hybrid coupler can achieve the high isolation between the two feed ports so that the power reflected from a mismatched port is transferred to the absorbing load ( $50 \Omega$  terminations). [41; 42]



a) Novel aperture feeding in [43]



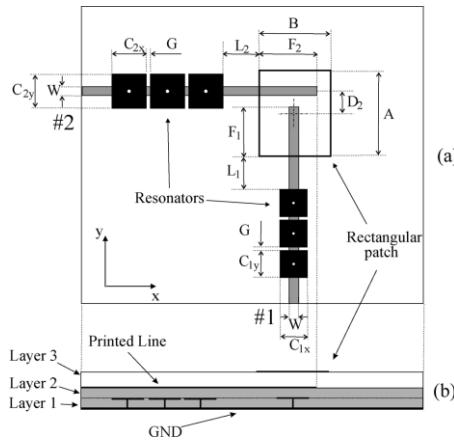
b) Slot coupling using striplines in [44]



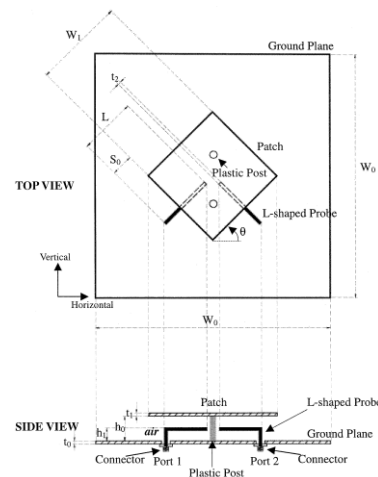
c) probe feeding with stacked patches [45]



d) Feeding separate patches using a power dividing circuit [41]



f) Proximity coupled feed [46]



g) L probe feed with shorted patch [47]

**Fig 6.3** Different feed configurations of dual polarized antennas

Dual polarized antenna designs in the past usually follow multilayer implementation. This is because multilayer implementations have several parameter options to enhance bandwidth [48] and increase isolation. Some of them follow electromagnetic feeding. Common electromagnetically fed antennas follow proximity or aperture coupling. Number of layers none the less should also be considered with respect to production complexity. [49]

### 6.2.2. Isolation

It is good if the orthogonal ports do not interfere with each other so better isolation is important. In [45], a parametric study has been studied to maximize isolation between the ports in probe coupled antennas and says isolation is improved for air gaps less than  $0.02\lambda_0$ . A method of using cross shaped aperture and modifying the aperture shape to reduce the isolation in aperture coupled antennas is also used in [30], [44], [50]. In [32], a patch with etched bars or grid is used to increase the isolation.

Most isolation methods involve aperture coupling. Aperture is also proved to be reliable and robust technique. However, aperture coupled feeds have the problem of high back-lobe radiation [47]. Fortunately this problem can be solved by placing a ground plane below the aperture [51], but this makes the antenna bulky [52]. Another method includes using proximity coupling [46], L shaped probe feed without shorted patch [47].

### 6.2.3. Bandwidth

Dual polarized antennas have been implemented for various bands. Example [30] for C band of 4GHz -8 GHz, [32] for center frequency of 1.3 GHz and for RFID band. [53], [41]. It has been mentioned in section x already that patch antennas have very narrow bandwidth. It gets worse for dual polarized antennas. This is because of the interference between the two inputs. Besides the techniques used to enhance the bandwidth of one port, affects the matching of the other.

Aperture coupled antennas have been reported suitable to implement wide band antennas [54]. There have been also other novel methods to enhance the bandwidth of dual polarized antennas. In [55] broadband baluns are used to increase the isolation and the bandwidth in turn. In [30] offset slots used for the same purpose.

### 6.2.4. Gain

Generally increasing size for patch antennas increases the maximum gain. In single polarized antennas, this can be achieved by increasing the width (the side field remains constant). This cannot be done for dual inputs since increasing the width for one input disturbs the oscillation for the other.

## 7. EXPERIMENTAL ANTENNA

It has been mentioned in the modal cavity model in chapter 3 that a patch has several resonance frequencies with the lowest resonance frequency being the dominant mode. Implementing dual polarized antennas in the same patch antenna for both horizontal and vertical polarizations means making use of more than one mode. For optimal size, volume and simplicity, a shape close to a square is used, so  $TM_{010}^x$  and  $TM_{001}^x$  should be considered as the dominant modes one for horizontal and the other for vertical polarization.

### 7.1. Designing Patch Size

The approximate patch size to start simulation is in the scale shown in patch antenna models in chapter 4. If the same frequency is used for the orthogonal inputs, the width and the length of the patch will be equal,

$$L, W = \frac{q}{2f_r \sqrt{\mu\epsilon}} \quad (7.1)$$

Where, as mentioned in chapter 3,  $q$  stands for the fringe factor,  $f_r$  stands for resonance frequency,  $\mu$  stands for substrate dielectric constant and  $\epsilon$  stands for electric permittivity. An equivalent equation that empirically calculates the fringe factor gives, [4].

$$L, W = \frac{c}{2f_r \sqrt{\epsilon_{eff}} \sqrt{\mu_0 \epsilon_0}} - 2\Delta L \quad (7.2)$$

where  $c$  is the speed of light,  $\mu_r$  stands for relative magnetic permeability,  $\epsilon_r$  stands for relative electric permittivity and  $f_r$  is the resonance frequency.  $\epsilon_{eff}$  is given as

$$\epsilon_{eff} = \frac{\epsilon_r + 1}{2} + \frac{\epsilon_r - 1}{2} \left[ 1 + 12 \frac{h}{W} \right]^{-\frac{1}{2}}, \quad \text{assuming } \frac{W}{h} > 1 \quad (7.3)$$

Where  $W$  is microstrip line thickness and  $h$  is the substrate thickness.  $L$  stands for the effective length  $= \frac{\lambda}{2}$

$$\Delta L = h * 0.412 \frac{(\epsilon_{eff} + 0.3) \left(\frac{W}{h} + 0.264\right)}{(\epsilon_{eff} - 0.258) \left(\frac{W}{h} + 0.8\right)} \quad (7.4)$$

The proposed antenna structure is given below

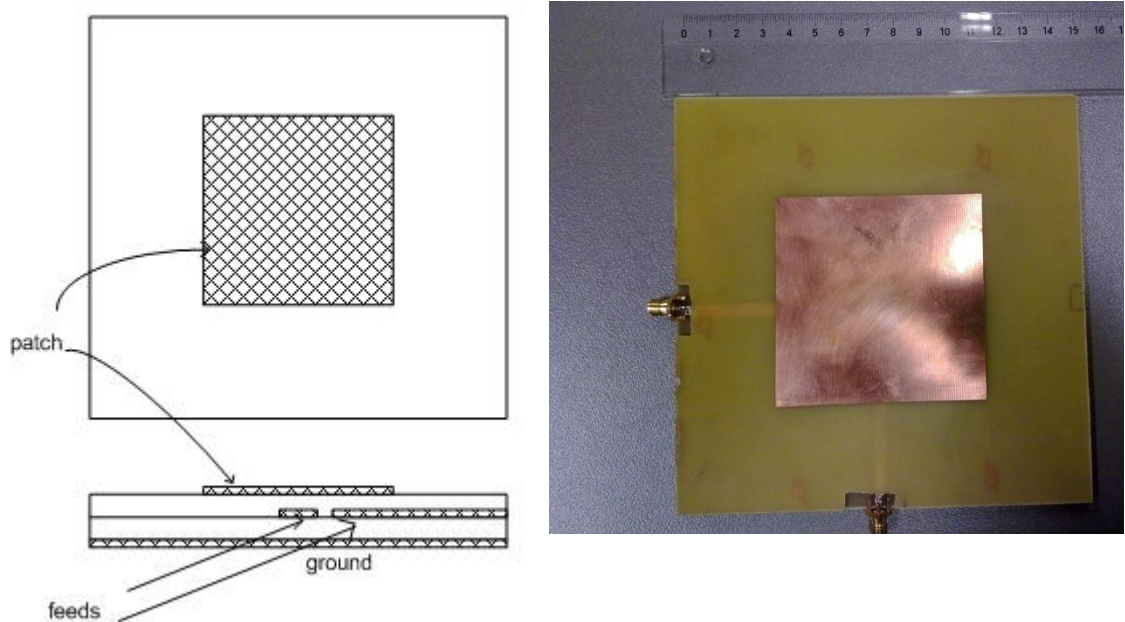


**Fig. 7.1** Proposed antenna top and side view (left) and picture (right)

The project is implemented with FR4 substrate with dielectric constant of 3.88. The antennas are designed to work in European RFID band so, for a center frequency of 867 MHz, the patch will have a size of 87.6 mm. This value is then optimized with the help of the simulation software.

With simulation software, the value of the patch calculated above is used and produces resonance at lower frequency. As a result, parametric sweep of the patch size was taken. Besides, the patch size, there were also other parameters of interest that help us optimize matching and affect the oscillation frequency. These factors include the length of each of the open stub feeds, The width of the open stub feeds and position of the feeds from each side.

Finally best matching with oscillation close to 867 MHz was obtained with patch length of 83 mm, stub feed length of 2.4 mm and length of 25 mm. Optimal result is obtained with stub ending 10 mm from center.

As shown in fig 7.1, there is no direct connection between the ports and the patch. Therefore the patch and the ports are electromagnetically coupled. Such coupling as mentioned in chapter 6 is called proximity coupling. The current density distribution can be seen to see how the inputs couple the patch. The figure below shows how each input couples the patch. Port 1 creates a surface current on the two

edges of the patch parallel to it. We see maximum current density on the sides with opposite phase. Similar but opposite phenomenon is shown for port 2.

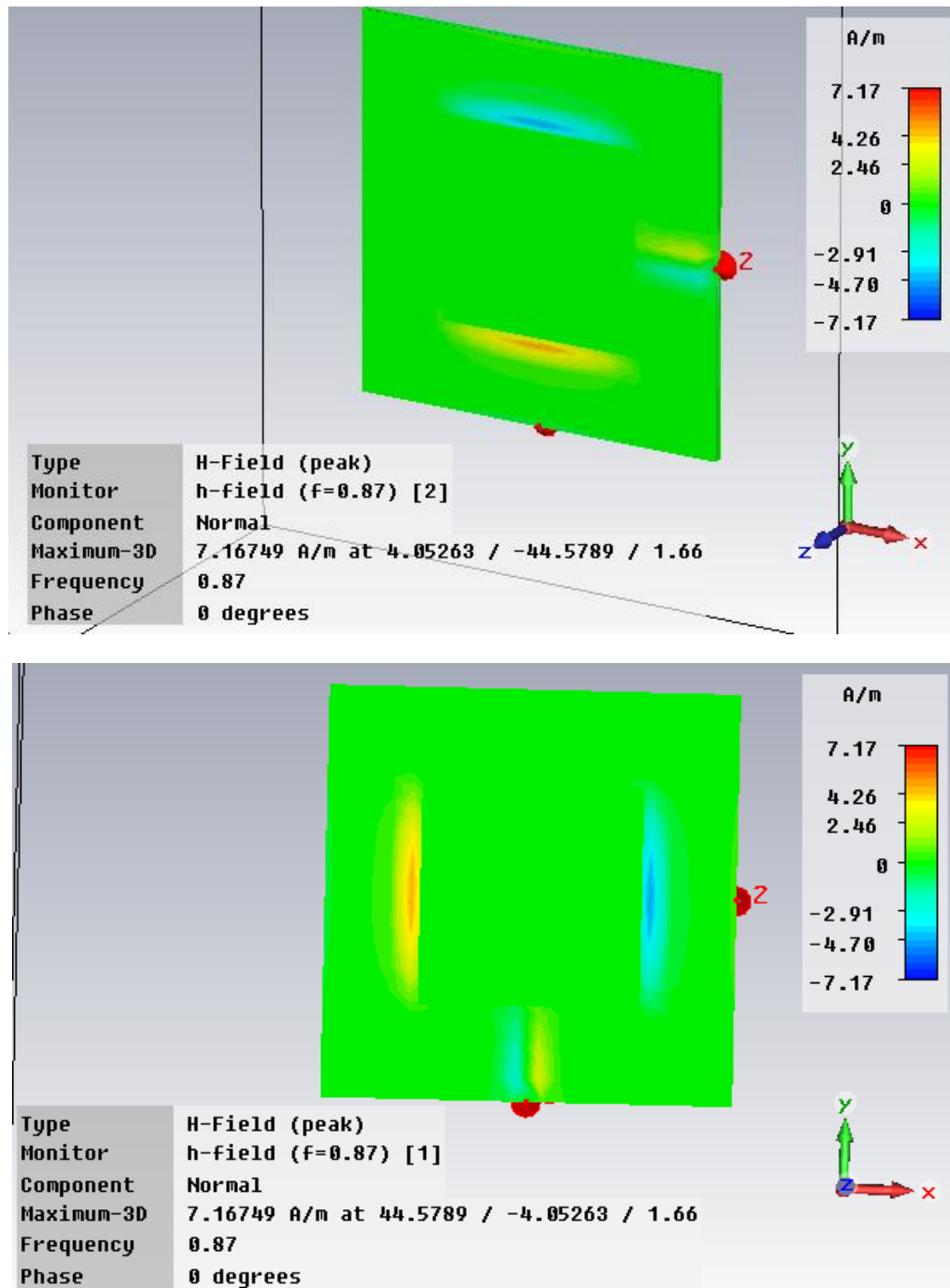


Fig 7.2 Current densities for port 1 (above) and port 2 (below)

## 7.2. Simulation Results

Simulation was carried out first with Empire XCell and then with CST Microwave Studio. The discussions that follow are based on CST Microwave Studio. As mentioned before, CST Microwave Studio follows FIT algorithm.

Simulation parameters include the scattered or S parameters, the far field radiation patterns and current densities.

Desired results can only be obtained with proper use of settings. The first setting is setting boundary conditions. There are electric, magnetic and open boundaries. Since, the antenna has a ground plane, the boundary in the bottom can be left electric or open (then using perfect electric conductor or metal layer). The other boundaries are left open. CST has an interesting feature of adjusting frequency ranges with the given boundary conditions or vice versa. Choice of mesh also affects the quality of results.

Simulation of the current densities is already shown in Fig. 7.2 above. For S parameters and radiation patterns, again the antenna of structure given in fig 7.1 is simulated. Two FR4 substrates of dielectric constant 3.88 and thickness 1.6mm are used. More information about the detail substrate parameters is given in appendix 2. The S parameter simulation results are given in the following figure.

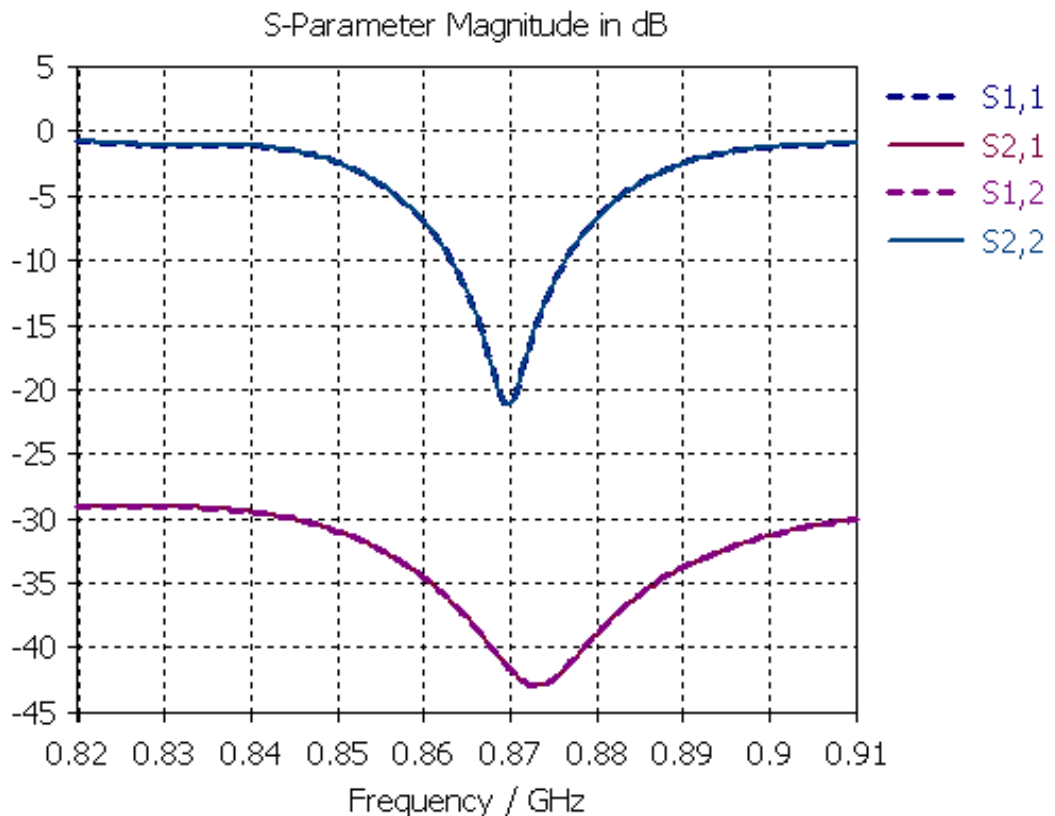


**Fig. 7.3** Simulated S parameters for antenna in fig. 7.1

We can see the simulated antenna with patch size 82 mm oscillates close to 868 MHz with 10 dB return loss bandwidth of about 10 MHz. Since the design is for just the European RFID band, which is 865-868 MHz, this bandwidth is enough. The simulated isolations in the scale of -40 dB. This value is ideal for efficient communication.

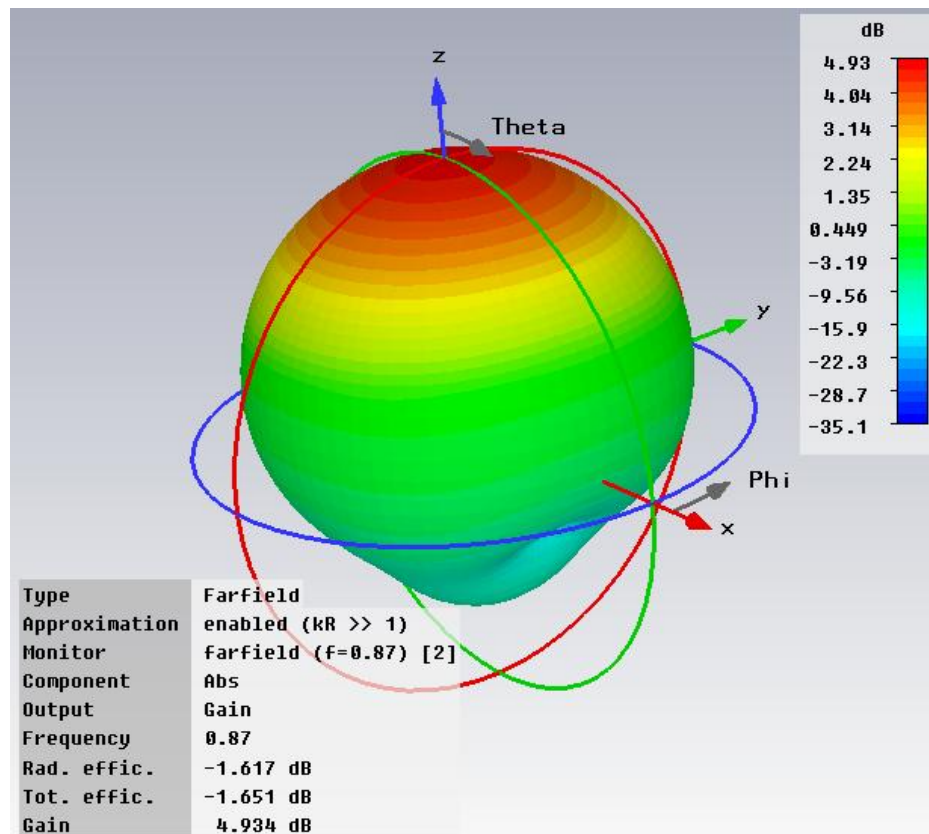
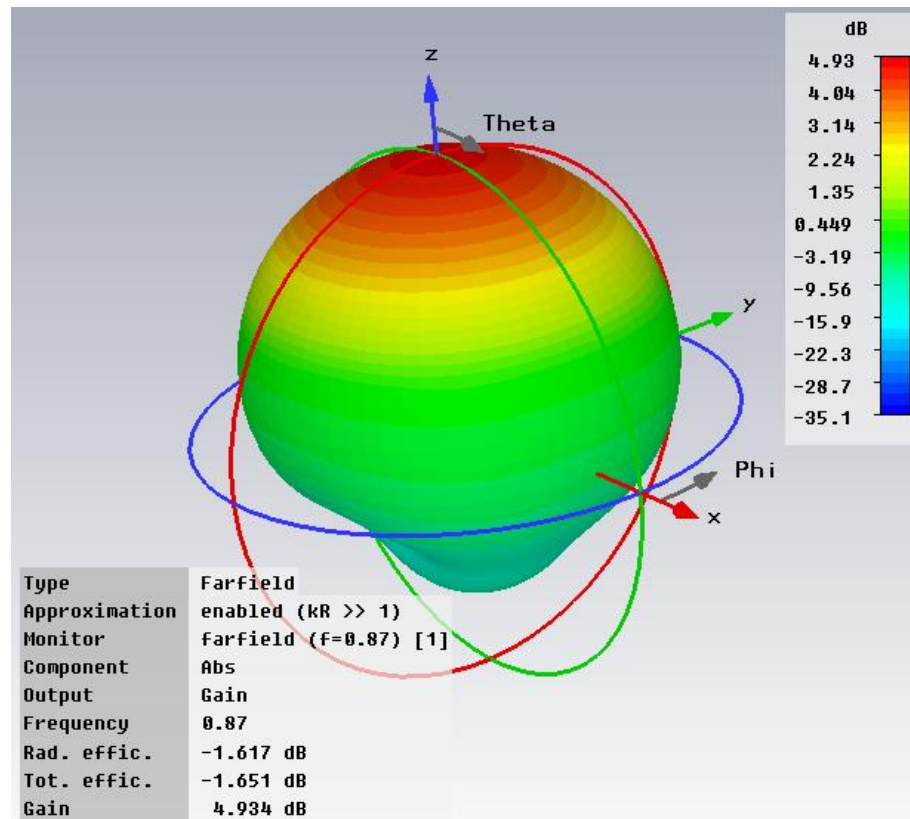


*Fig. 7.4* The simulated 3D pattern for port 1 (above) and port 2 (below)

The absolute gain patterns are given in polar 1D plot (for E- and H-planes) and in 3D. The 3D plots are shown in figure 7.4 above. The plot is taking considering an antenna oriented in the xy-plane. The plot above is for feed 1 and the plot below is for feed 2. Feed 1 is in y direction and feed 2 is in x direction. As can be seen from the result both have maximum gain close to 4.93 dBi oriented in +z direction.

There are several choice of axis. From these, spherical and Ludwig 3 coordinates seem more relevant. To see polarization gains, Ludwig 3 coordinate system is better. It was discussed in chapter 3 that the horizontal and vertical polarization components can be matched to the cross polarization and co-polarization. Gains in E plane and H plane results are shown below in the same picture and for each port.

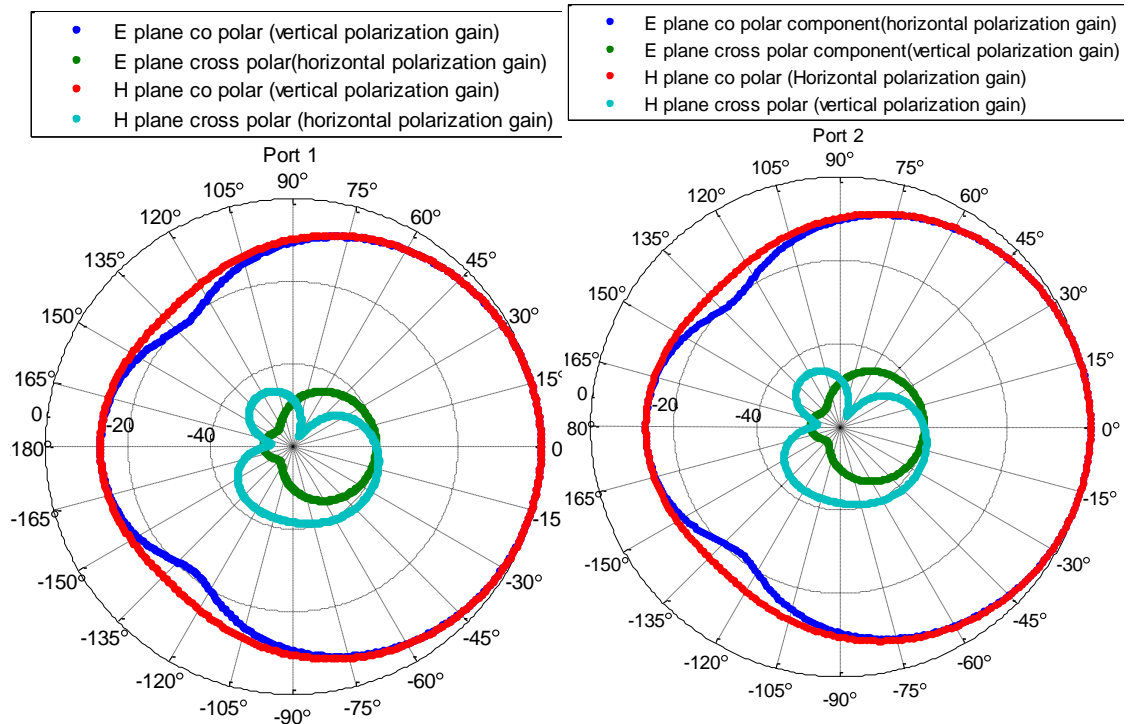


**Fig. 7.5** Comparison of normalized absolute gains, co polar and cross polar components for both ports

From figure 7.5 above, it can be understood that (port 1) has very low Ludwig 3 horizontal polarization gain and higher Ludwig 3 vertical gain with a ratio up to 40 dB. Therefore, for this port, horizontal gain is the cross polar gain and vertical gain is co polar gain. On the contrary, port 2 has high Ludwig 3 horizontal gain or co-polarization and low Ludwig 3 vertical gain which is the cross polarization.

### 7.3. Measurement Results

The measured results in turn include S parameters taken from Vector Network Analyzer (VNA) and antenna radiation patterns taken from Satimo Starlab. The VNA is interfaced with a computer that has Advanced Design System (ADS) software where data can be written to. Since the antenna has two ports, a complete two port calibration has to be carried out for the VNA. After that, the instrument will be ready to measure both return losses and isolations.

Satimo Starlab is an antenna pattern measuring tool that processes the near field data to come up with far field radiation patterns. It is equipped with passive starlab and Satenv softwares to process and export measurement results. These measurement set ups are shown in fig 7.6 below [56]. Similarly, calibration should to be done for Satimo Starlab as well for specified frequency range and resolution. Calibration is done with certain reference antenna such as dipole or horn antenna.



*Fig. 7.6 Measurement set up for S parameters by VNA (left) and Satimo Starlab (right)*

The first measurements were carried out for S parameters of the antennas. As mentioned before S parameters define the power transmission and reflection characteristics of an antenna. For microstrip antennas, since they have very narrow bandwidth, a slight error in estimating the dielectric constant, patch size, other parameters such as stub length and thickness shift the oscillation frequency. After two prototypes, the correct oscillation frequency is obtained as shown in fig. 7.7 and fig. 7.8 below.

$S_{11}$  and  $S_{22}$  stand for return losses accounting for power reflected back to the feed. Ideal values are linearzero.  $S_{21}$  and  $S_{12}$  are isolations and indicate power transmitted from one port to the other. Again ideal case is zero (infinite negative in dB). [8]

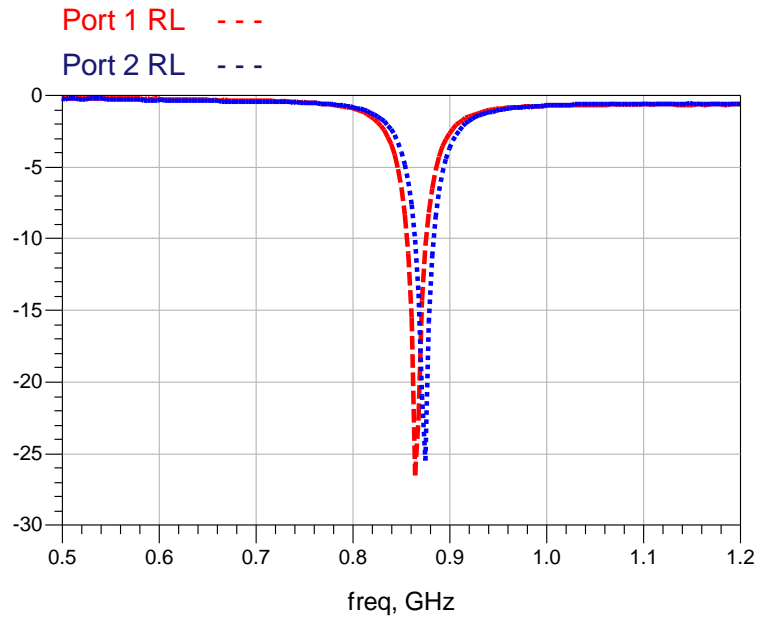


*Fig. 7.7 Measured return losses*

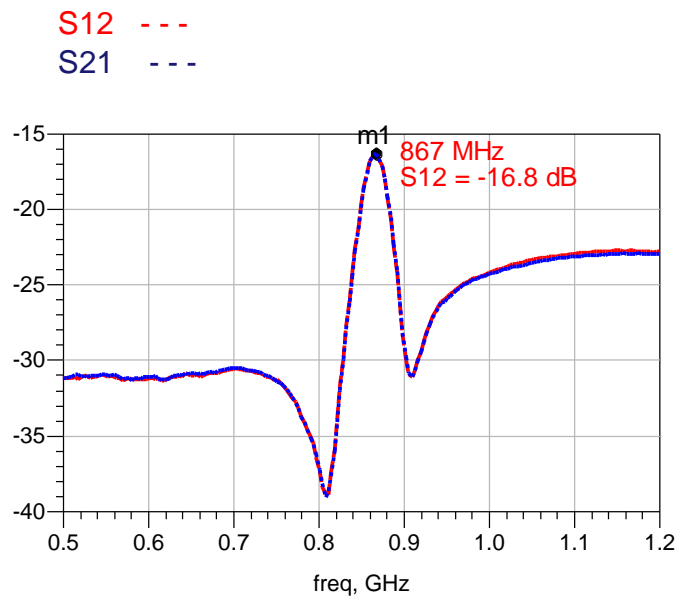


*Fig. 7.8 Measured input port isolations*

The return losses resemble the simulated values. Unlike the simulation, the isolation has decreased from -40 dB up to -16.3 dB at 867.5 MHz. For the radiation patterns first is given measured 3D absolute gain.

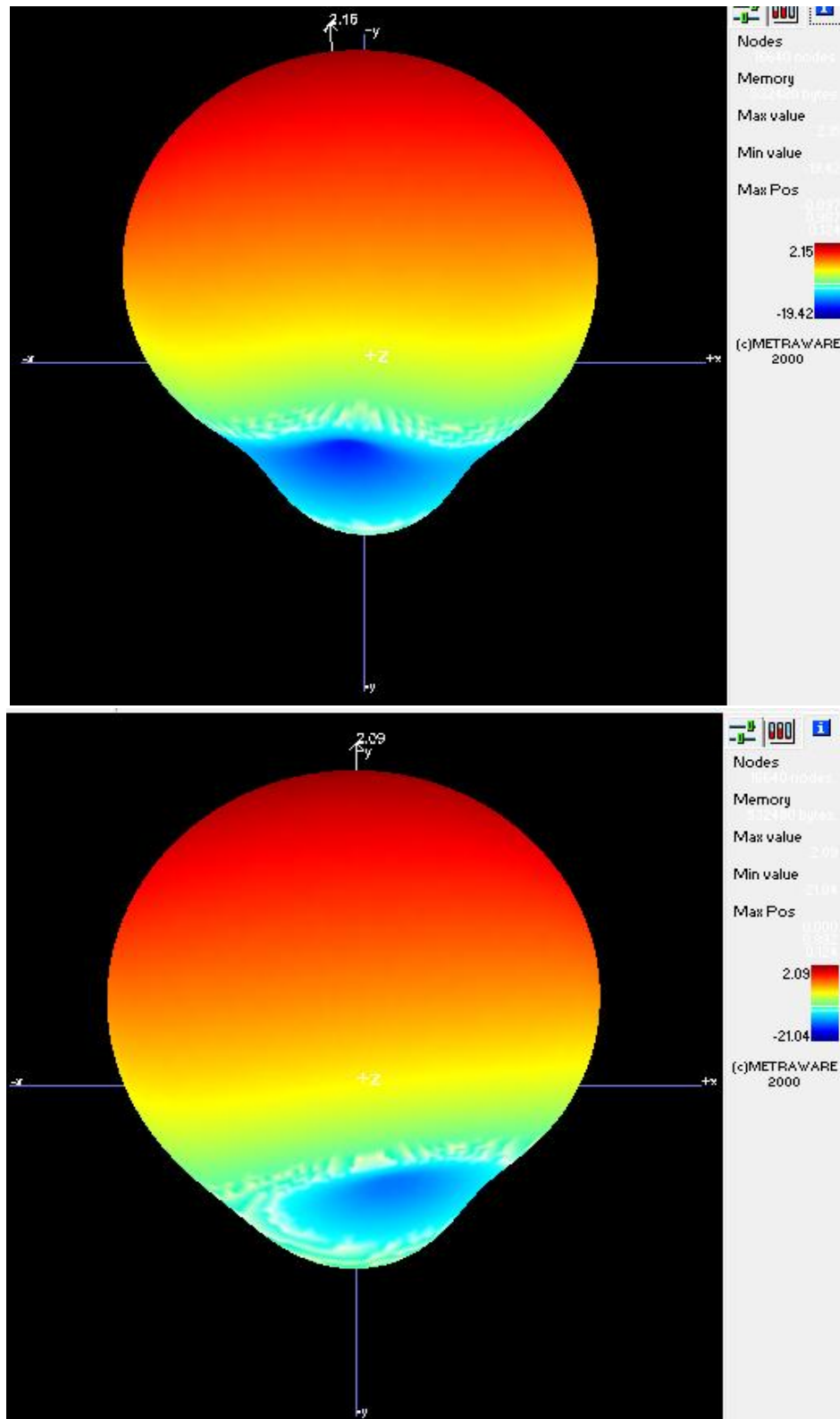


*Fig. 7.9 Measured 3D gain patterns port 1 (above) and port 2 (below), maximum 2.15 dBi and 2.09 dBi respectively*

Then polar 1D (E- and H- plane) plots are given for absolute gain, gain  $\phi$  and gain  $\theta$ . Again the results for one of the ports are given for each antenna for simplicity.

From fig. 7.9 above, it can be seen that the antennas show reduced gain from that of the simulated but generally exhibit similar directive pattern.

Measured radiation patterns in comparison with the simulated patterns for E and H planes are shown in the figure below.

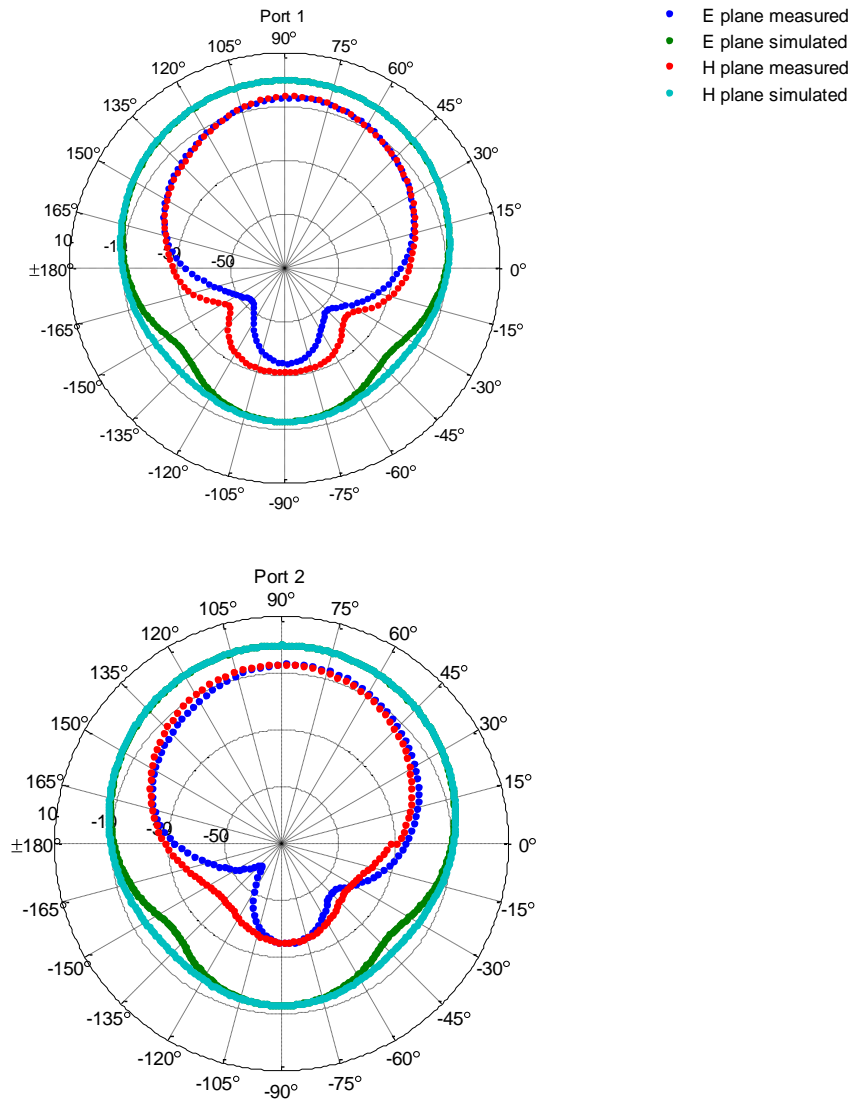


**Fig. 7.10** Comparison of measured and simulated polar gain (dBi) patterns at 867 MHz for port1 (above) and port 2 (below)

## 7.4. Modification of the Basic Antenna

An idea of implementing slots on ground was proposed to enhance bandwidth and isolation. The ground is slotted as shown in the figure below.

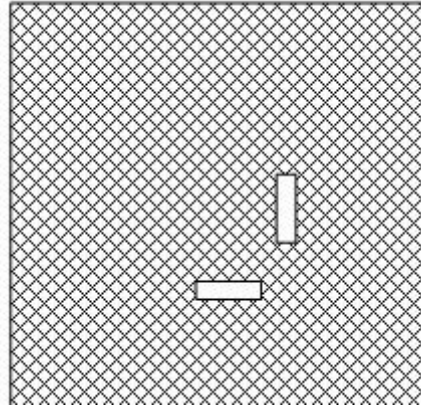


*Fig. 7.11 Modification from the antenna in fig 7.1 with slots at the ground plane*

The positions and width of slots were parameters of the simulation. The simulation result was only slightly better in improving the bandwidth and the gain. Not much was improved.

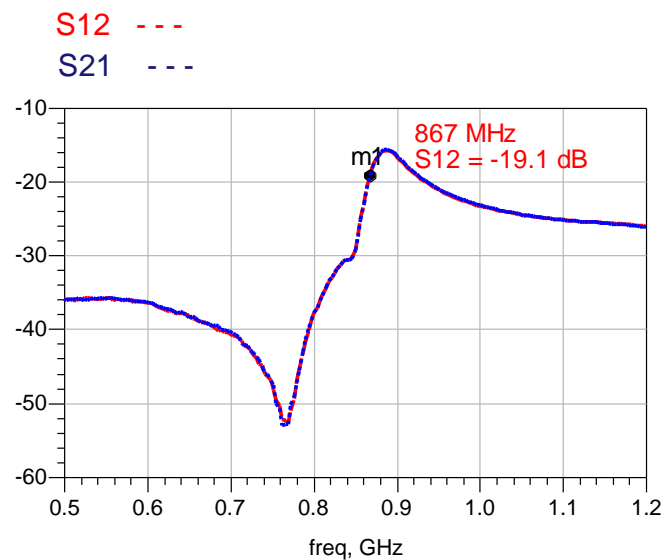


*Fig. 7.12 Measured isolations for modified antenna*

Nevertheless, the implemented antenna shows a better isolation and more gain with better directional characteristics. The advances in isolation can be seen from the figure below. Earlier it was only 16.5 dB at 867.5 MHz; now it is 19.4 dB.

Looking at the radiation pattern for the modified antenna, the pick gain has improved as shown in the figure below. The maximum gain is about 2.7 dBi, which is an increase of about 0.5 dB from the basic antenna. The shape however, has deteriorated to a certain extent. Again polar plots gain plots for simulated and measured values are given below.

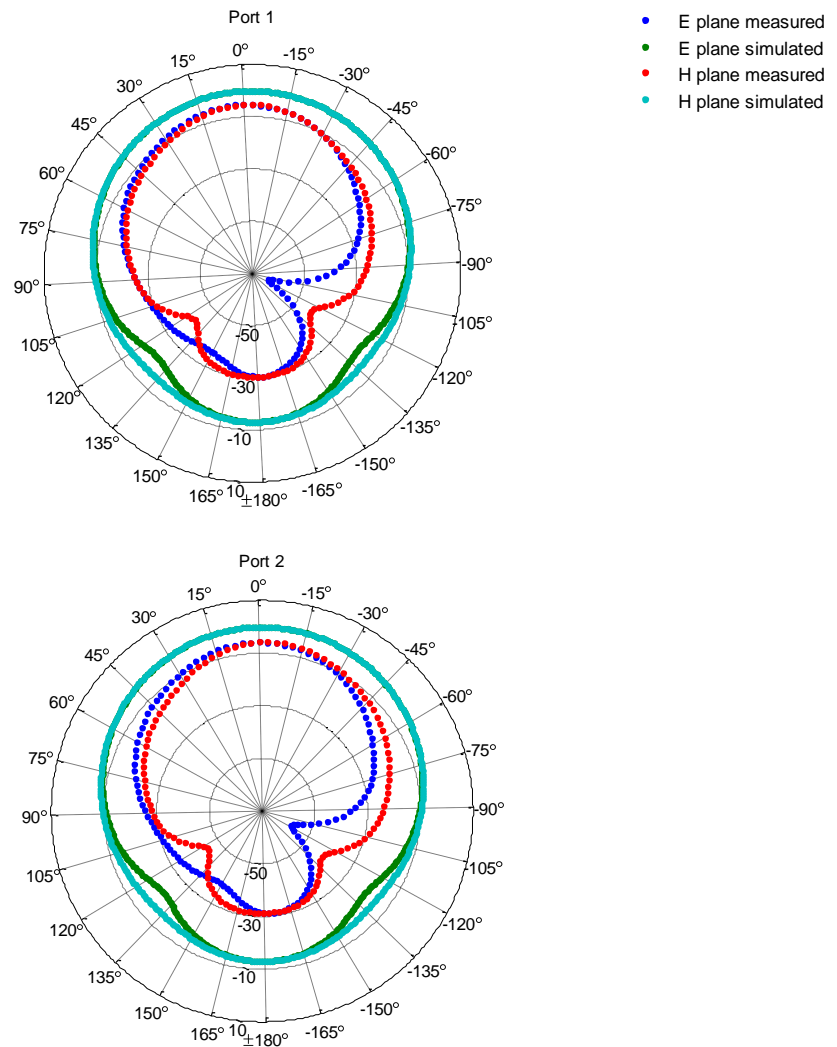


**Fig. 7.13** Comparison of measured and simulated polar gain (dBi) patterns of the modified antenna at 867 MHz

## 8. CONCLUSIONS

RFID is a fast emerging identification system and it has been preferred to other systems for applications that need bigger read range with good data density, better security and high speed. Passive UHF RFID, being rather common RFID technology, promises simple and long life tags as it consists of no battery in the tags. Therefore, up to several meters of read range have been possible using RFID.

Nevertheless, the need for increased read range and simpler tags still remains. This thesis deals with this issue by presenting options for energy efficient RFID systems from a reader point of view- specifically improving reader antenna.

It has been shown in the thesis that most tag antennas are linearly polarized while readers are circularly or linearly polarized. Comparison of polarization loss factor was then estimated for each case. A major loss happens when linearly polarized reader antennas are used. In this scenario, the tags can only be read if their orientation has some component in the direction of the reader antenna. It has also been shown that circularly polarized antennas have fields that rotate a plane and they can only have polarization match of 0.5 in average.

Therefore, along with other proposals, dual polarized patch antennas were proposed. The proposed antennas will improve the reverse (tag to reader) communication with no receiver features but the forward (reader to tag) communication can also be improved with the suggested receiver feature that adapts to the orientation of the tag.

General ideas for the design were taken from various books of antenna and microwave engineering and journals from IEEE. The antennas were based on microstrip patch antennas. Then, simulations were carried out using Empire XCell and CST Microwave Studio. Two antennas were implemented for comparison. The implementation was carried out in RF work shop laboratory in TUT.

The antennas were tested first using VNA for matching and needed oscillation frequency. Further measurements for radiation patterns were carried out in Satimo Starlab. Comparison was then carried out by exporting files and plotting with Matlab. The results for matching are shown in the thesis. The results from simulation and measurement generally match. Oscillation happens at the right frequency and the antennas have  $> 10$  dB return loss in the European RFID band, which has been the design goal. The measured radiation patterns also match with the simulated except some reduction in gain. Inaccurate simulation, antenna practicalities and huge measuring device tolerance ( $\pm 1$  dB) could be the possible reasons for gain reduction.

The simulations and measurements were carried for both ports of the antennas and the two ports show orthogonal polarizations. Thus, the antennas are dual polarized. Simulated cross polarization levels are shown, and are lower than -30 dBi. The antennas have minimum input port isolations of 16.5 dB and 19 dB. This figure is poor as compared to many antennas dual polarized antennas.

The antennas have not been yet tested in an RFID system. But generally, it has been shown that with further gain optimization and making specific changes to meet required applications, the suggested dual polarized antennas can be used in RFID systems to improve efficiency.

## REFERENCES

- [1] Noyan Kinayman, *Modern Microwave Circuits*. Boston: Artech House, Inc, 2005.
- [2] David K. Cheng, *Field and Wave Electromagnetics*.: ADDISON-WISLEY PUBLISHING COMPANY, 1992.
- [3] Constantine A. Balanis, *Advanced Engineering Electromagnetics*.: John Wiley & Sons, 1989.
- [4] Constantine A. Balanis, *Antenna Theory Analysis and Design*. Hoboken: John Wiley & Sons, Inc., 2005.
- [5] Long Gen Zheng ; Chao Liu ; Yu Zhong Jiang ; Zhi Gang Zhang ; Wen Xun Zhang, "Re-examine the Limitation of the Complex Poynting Theorem," in *Environmental Electromagnetics, The 2006 4<sup>th</sup> Asia-Pacific Conference on* , 2006, pp. 662 - 665.
- [6] Warren L. Stutzman, *Antenna Theory and Design*.: John Wiley & Sons Inc., 1998.
- [7] "IEEE Standard Definitions of Terms," 1993.
- [8] Pavel Bretchko Reinhold Ludwig, *RF Circuit Design: Theory and Applications*. NJ: Prentice Hall, 2000.
- [9] K. Carver and J. Mink, "Microstrip Antenna Technology," pp. 2 - 24, 1981.
- [10] Daniel M. Dobkin, *The RF in RFID*. Burlington: Elsevier Inc., 2008.
- [11] A. Ludwig, "The definition of cross polarization," in *Antennas and Propagation, IEEE Transactions*, 1973, pp. 116-119.
- [12] CST Microwave Studio, Far field Overview, CST software help.
- [13] R.P. Ray Girish Kumar, *Broadband Microstrip Antennas*. Norwood: Artech House, Inc., 2003.
- [14] E. Budak et al., "Microstrip patch antenna for RFID applications," in *RFID Euroasia*, 2007, pp. 1-3.
- [15] David M. Pozar, *Microwave Engineering*.: John Wiley & Sons, 2005.

- [16] CST. (2010) [Online]. <http://www.cst.com>
- [17] Empire Xcell. (2008) [Online]. <http://www.empire.de>
- [18] A. Taflove, "Application of the Finite-Difference Time-Domain Method to Sinusoidal Steady-State Electromagnetic-Penetration Problems," *IEEE Journals*, pp. 191 - 202, 1980.
- [19] J. R., P. S. Hall, James, *Handbook of Microstrip Antennas, Vol. 1*. London: Peter Peregrinus Ltd., 1989.
- [20] A. G. Lind, Derneryd, "Extended Analysis of Rectangular Microstrip Resonator Antennas, Vol. AP-27," in *IEEE Trans. Antennas Propagation*, 1979, pp. 846-849.
- [21] Klaus Finkenzeller, *RFID Handbook Fundamentals and Applications in Contactless Smartcards and Identification*. Wiltshire: John Wiley & Sons Inc., 2003.
- [22] Confidex. [Online]. <http://www.confidex.fi/why-rfid/benefits-from-rfid>
- [23] P-J Lin, H-C Teng, H-J Muang, and M-K Chen, "Design of patch antenna for RFID reader applications," in *Anti-counterfeiting, Security, and Identification in Communication*, 2009, pp. 193-196.
- [24] Alejandro Aragon Zavala Simon R. Sauders, *Antennas and Propagation for Wireless Communication Systems*, 2<sup>nd</sup> ed. Wiltshire, UK: Wiley and sons inc.
- [25] Braid A.R. Ibrahim and Mustapha C.E. Yagoub, "Practical novel design component of microstrip patch slot antenna MSPSA for RFID Applications," in *Electrical and Computer Engineering (CCECE), 2010 23<sup>rd</sup> Canadian conference on Digital Object identifier*, 2010, pp. 1-5.
- [26] Hao Wei Kwa, Xianming Qing, and Zhi Ning Chen, "Broadband single-fed single-patch circularly polarized antenna for UHF RFID applications," in *Antennas and Propagation Society International Symposium*, 2008, pp. 1-4.
- [27] H-S Tae, K-S Oh, M-Q Lee, J-W Yu D-Z Kim, "Helical reflector antenna with a wideband CP for RFID reader," in *Microwave conference*, 2009, pp. 1032-1035.
- [28] N. Misran, M.T. Islam, L.L. San, and R. Azim, "Dual-polarized patch antenna for wireless communication," in *Electrical Engineering and Informatics, 2009*, 2009, pp. 703-706.

- [29] Zhishu Xu and Xiuping Li, "Aperture coupling two-layered dual-band RFID reader antenna design," in *Microwave and Millimeter Wave Technology, 2008, vol.3*, 2008, pp. 1218-1221.
- [30] M. Edimo, A. Sharaiha, and C. Terret, "Optimized feeding of dual polarized broadband aperture-coupled printed antenna," in *Electronics Letters*, 1992, pp. 1785-1787.
- [31] C-L Zhang and B.J. Hu, "A Novel koch Fractal Microstrip Antenna Coupled with H-shaped Aperture for RFID Reader," in *Wireless Communications, Networking and Mobile Computing, 2008*, pp. 1-3.
- [32] L. Habib, G. Lpssoavas, and A. Papiernik, "Cross-shaped patch with etched bars for dual polarisation," in *Electronics Letters*, 1993, pp. 916-918.
- [33] B. Yang and Q. Feng, "A patch antenna for RFID reader," in *Microwave and Millimeter Wave Technology, 2008*, pp. 1044-1046.
- [34] Y. S. Boo, Nasimuddin, Z. N. Chen, and A. Alphones, "Broadband circularly polarized microstrip antenna for RFID applications," in *Microwave Conference, 2009*, pp. 625-628.
- [35] W-S Chen and Y-C Huang, "A novel RFID reader antenna with circular polarization operation ," in *Application of Electromagnetism and Student Innovation Competition Awards (AEM2C), 2010*, pp. 117-120.
- [36] Z. Xu and X. Li, "Aperture coupling two-layered dual-band RFID reader antenna design," in *Microwave and Millimeter Wave Technology, 2008*, pp. 1218-1221.
- [37] Z. N. Chen and H.L Chung X.Qing, "A Universal UHF RFID Reader Antenna," in *Microwave Theory and Techniques, IEEE Transactions*, 2009, pp. 1275-1282.
- [38] Nasimuddin, K. P. Esssele, and A.K. Verma, "Improving the axial-ratio bandwidth of circularly polarized stacked microstrip antennas and enhancing their gain with short horns," in *Antennas and Propagation Society International Symposium, 2006*, pp. 1545-1548.
- [39] X. He, S. Hong, H. Xiong, Q. Zhang, and E.M.M. Tenzeris, "Design of a Novel High-gain Dual-Band Antenna for WLAN Applications," in *Antennas and Wireless Propagation Letters, 2009*, pp. 798-801.
- [40] L. Ukkonen, L. Sydanheimo, and M. Kivikoski, "Effects of metallic plate size on the performance of microstrip patch-type tag antennas for passive RFID ," in

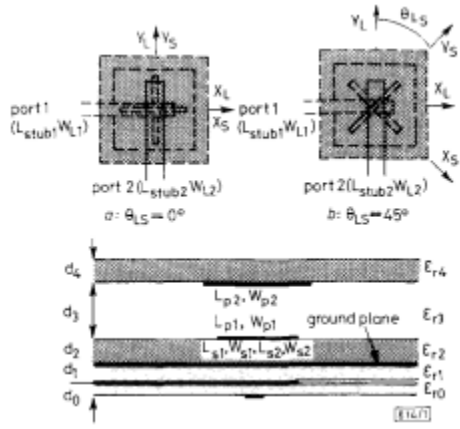
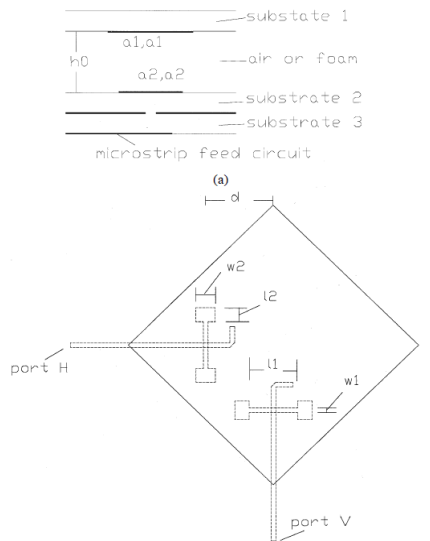
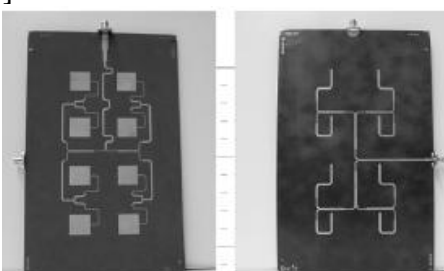
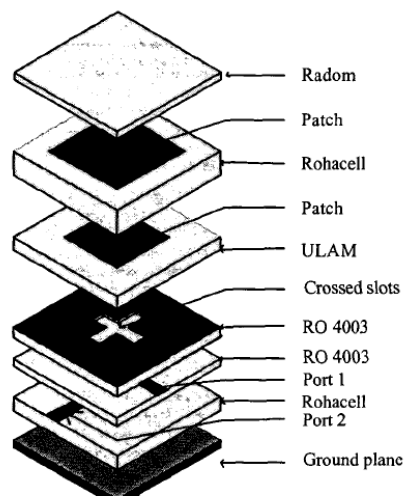
*Antennas and Wireless Propagation Letters*, 2005, pp. 410-413.

- [41] M. S. Mhod, M.K. Suaidi, M. Abdul Aziz, and M.F.A. Kadir, "Dual polarization microstrip patch array antenna for WLAN application," in *Antennas and Propagation, 2009, EuCAP 2009 3<sup>rd</sup> European Conference*, 2009, pp. 1264-1268.
- [42] H.L Chung, X. Qing, and Z. N. Chen, "Broadband circularly polarized stacked patch antenna for UHF RFID Applications," in *Antennas and Propagation Society International Symposium*, 2007, pp. 1189-1192.
- [43] A. Adrian and D.H. Schaubert, "Dual aperture-coupled microstrip antenna for dual or circular polarization," pp. 1226-1228, 1987.
- [44] M. Yazamaki, E. T. Rahardjo, and M. Haneishi, "Construction of a slot-coupled planar antenna for dual polarization," in *Electronics Letters*, 1994, pp. 1814-1815.
- [45] S. Gupta, M. Ramesh, and A.T. Kalghatgi, "Parametric studies on isolation in probe-fed dual polarized microstrip antennas," in *Wireless Technology*, 2005, pp. 483-485.
- [46] L.Inclan-Sanchez, -L. Vazquez-Roy J, and E. Rajo-Iglasias, "High isolation proximity coupled Multilayer Patch antenna for Dual-Frequency Operation," in *Antennas and propagation*, 2008, pp. 1180-1183.
- [47] H. Wong, K-L. Lau, and K-M Luk, "Design of dual-polarized L-probe patch antenna arrays with high isolation," in *Antennas and propagation*, 2004, pp. 45-52.
- [48] M. Edimo, A. Sharaiha, and C. Terret, "Optimized Feeding of Dual Polarized Broadband Aperture Coupled Antenna," *IET Journals* , pp. 1785 - 1787, 1992.
- [49] M. Yamazaki, E.T. Rahardjo, and M. Haneishi, "Construction of a slot coupled planar antenna for dual polarization," 1994.
- [50] P. Brachat and J.M. Baracco, "Dual-polarization slot-coupled printed antennas fed by stripline," in *Antennas and Propagation*, 1995, pp. 738-742.
- [51] H. Wong, K-L Lau, and K-M Luk, "Design of dual-polarized L-probe patch antenna arrays with high isolation," in *Antennas and Propagation*, 2004, pp. 45-52.
- [52] F. Klefenz and A. Dreher, "Aperture-coupled stacked microstrip antenna with dual polarization and low back-radiation for X-band SAR applications," in

*Radio and Wireless Conference*, 2000, pp. 179-182.

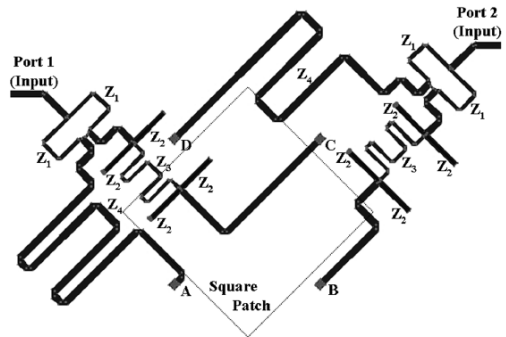
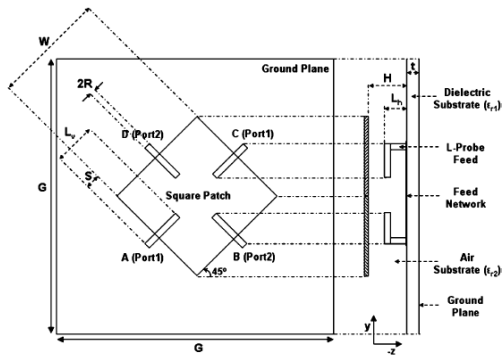
- [53] S.K. Padhi, N.C. Karmakar, and C.L. Law, "Dual polarized reader antenna array for RFID application ," in *Antennas and Propagation Society International Symposium*, 2003, pp. 265-268.
- [54] S. Heinonen, A. Lehto, and A.V. Raisanen, "Simple broadband dual-polarized aperture coupled microstrip antenna," in *Antennas and Propagation Society*, 1999, pp. 1228-1231.
- [55] K-W Khoo' U-X Guo, "Wideband Dual-polarized Patch Antenna," in *Communications Systems*, 2006, pp. 1-5.
- [56] Satimo. [Online]. [www.satimo.com/contents/products/starlab](http://www.satimo.com/contents/products/starlab)
- [57] L. W. Li, M. S. Leong, T. S. Yeo S. Gao, "A Broad-Band Dual-Polarized Microstrip Patch Antenna," in *Antennas and Propagation*, 2003 , pp. 898 - 900.
- [58] I. Acimovic, D.A. McNamara, and A. Petosa, "Dual-Polarized Microstrip Patch Planar Array Antennas With Improved Port-to-Port Isolation ," in *Antennas and Propagation, IEEE Transactions on* , 2008, pp. 3433-3439.
- [59] Hong-Twu Chen, Tzung-Wern Chiou, and Kin-Lu Wong, "Broadband dual-polarized patch antennas with hybrid feeds for 1800-MHz band operation," in *Antennas and Propagation Society International Symposium, 2001. IEEE*, 2001, pp. 102 - 105 vol.1.
- [60] D. H. Schaubert Pozar, "Microstrip Antennas: The Analysis and Design," in *IEEE Press*, New York, 1995.
- [61] Norwegian Institute of Science and Technology. [Online]. [www.ntnu.no](http://www.ntnu.no)

## APPENDIX 1: SURVEY OF KEY PARAMETERS OF SOME DUAL POLARIZED ANTENNAS FROM IEEE PAPERS

<p>[30]</p>  <p>Top view (above), side view (below)</p> <p><b>Total Dimensions</b> Total 0.8 X 1.5 X 15 mm<sup>3</sup></p> <p><b>Material</b> Five layers <math>\epsilon_{r1,2,4} = 2.55</math>  <math>\epsilon_{r3} = 1</math> (air)  <math>\epsilon_{r0} = 2.2</math></p> <p><b>VSWR &lt; 2 BW</b> 4-8 GHz ; 15-30%</p> <p><b>S<sub>21</sub>, - S<sub>12</sub></b> 22dB → -28 dB</p> <p><b>Cross Polar level</b> -17 → -22 dB</p> <p><b>Feed Method</b> Aperture</p>	<p>[57]</p>  <p>Top view (above), side view (below)</p> <p><b>Dimensions</b> Shown above</p> <p><b>Material</b> Three substrates  <math>\epsilon_{r1,2} = 2.33, \epsilon_{r3} = 2.2</math>          and air gap</p> <p><b>VSWR &lt; 2 BW</b> 2.5-3 GHz ; 20%</p> <p><b>S<sub>21</sub>, - S<sub>12</sub></b> &gt; 30 dB</p> <p><b>Cross Polar level</b> -23 dB (both E and H plane)</p> <p><b>Feed Method</b> Aperture</p> <p><b>Max. Gain</b> 7.5 dBi</p>
<p>[58]</p>  <p>2x4 array</p>	<p>[52]</p>  <p><b>Dimensions</b> Total 0.8 X 1.5 X 15 mm<sup>3</sup></p> <p><b>Material</b> Five layers <math>\epsilon_{r1,2,4} =</math></p>

	<p>2.55  <math>\epsilon_{r3} = 1</math> (air)  <math>\epsilon_{r0} = 2.2</math></p> <p><b>VSWR&lt;2 BW</b> 20%  <b><math>S_{21}, - S_{12}</math></b> More than 20 dB  <b>Cross Polar level</b> -17→-22 dB  <b>Feed Method</b> Aperture  <b>Max. Gain</b> 7 dBi (either port)</p>
<p>Individual patch</p>	
<p><b>Dimensions</b></p>	<p>Individual patch <math>l \times w = 17.05 \times 16.03 \text{ mm}^2</math></p>
<p><b>Material</b></p>	<p>Two layers  <math>\epsilon_{r1,2} = 2.2</math>  <math>h_2 = 0.5 \text{ mm}</math> <math>h_1 = 1.6 \text{ mm}</math></p>
<p><b>VSWR&lt;2 BW</b></p>	<p>2.3%; center 5.505 GHz</p>
<p><b><math>S_{21}, - S_{12}</math></b></p>	<p>-34dB → -45 dB</p>
<p><b>Cross Polar level</b></p>	<p>NA</p>
<p><b>Feed Method</b></p>	<p>Aperture for vertical feed and direct feed for horizontal</p>

[55]



**Dimensions**

**Material**

**VSWR<2 BW**

**$S_{21}, - S_{12}$**

**Cross Polar level**

**Feed Method**

**Max. Gain**

Total area = 300X300 mm<sup>2</sup>

R04008 substrate  $\epsilon_{r1} = 3.88$ ,  $t = 0.8 \text{ mm}$  containing feed network; four L probe feeds couple the patch suspended at  $H = 24 \text{ mm}$

34%, 1.67-2.31 GHz

More than 20 dB

-11→-28 dB

L probe

~7 dBi (either port)

## APPENDIX 2: FR4 SUBSTRATE MATERIAL PARAMETRES

FR4 Laminate	
FR4 Laminate substrate thickness	1.6 mm
Copper layer thickness	35 $\mu\text{m}$
Dissipation factor	35
Dielectric constant	3.86
Solderbath resistance (260 <sup>0</sup> C)	20 seconds
Resist Thickness	5 microns
Spectral Response	350-450 nm
UV Characteristics	
UV light energy requirement	50 mi/cm
Exposure Time	90 -120 seconds
Shelf life	1 year at 15-20 <sup>0</sup> C
Developer	3204996
Etchant	Ferric Chloride Pallets or Liquid and Fine Etch Crystals